ALLOY CATALYSTS WITH MONOLITH SUPPORTS FOR METHANATION OF COAL-DERIVED GASES, PHASE 1. ANNUAL TECHNICAL PROGRESS REPORT, APRIL 22, 1975--APRIL 22, 1976

BRIGHAM YOUNG UNIV., PROVO, UTAH

06 MAY 1976

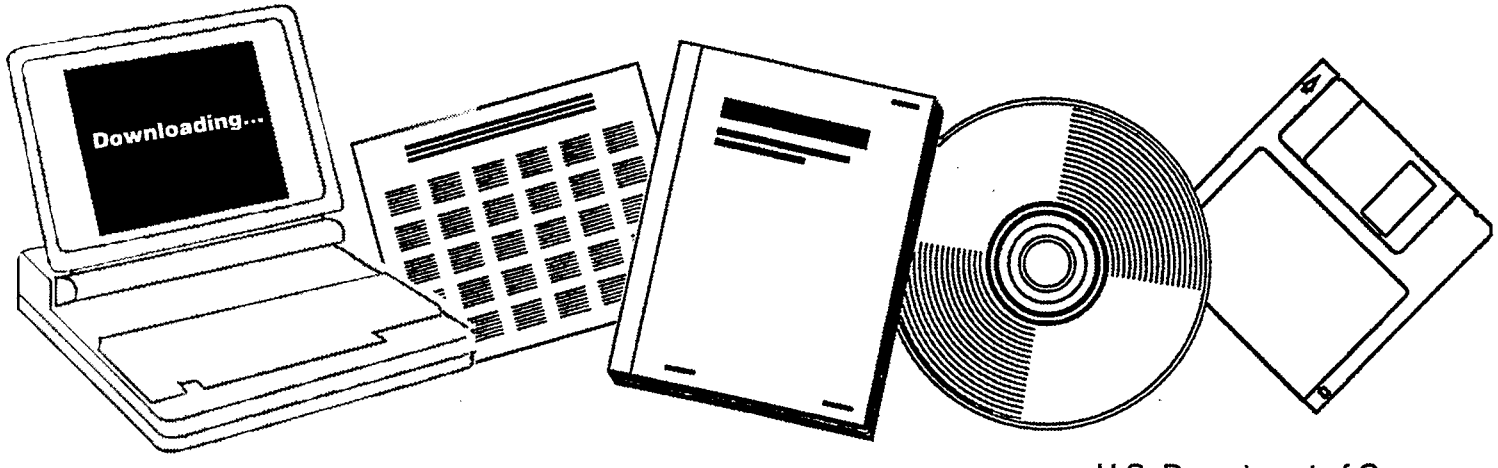

One Source. One Search. One Solution.

NTIS

Providing Permanent, Easy Access to U.S. Government Information

National Technical Information Service is the nation's largest repository and disseminator of government-initiated scientific, technical, engineering, and related business information. The NTIS collection includes almost 3,000,000 information products in a variety of formats: electronic download, online access, CD-ROM, magnetic tape, diskette, multimedia, microfiche and paper.

Search the NTIS Database from 1990 forward

NTIS has upgraded its bibliographic database system and has made all entries since 1990 searchable on **www.ntis.gov.** You now have access to information on more than 600,000 government research information products from this web site.

Link to Full Text Documents at Government Web Sites

Because many Government agencies have their most recent reports available on their own web site, we have added links directly to these reports. When available, you will see a link on the right side of the bibliographic screen.

Download Publications (1997 - Present)

NTIS can now provides the full text of reports as downloadable PDF files. This means that when an agency stops maintaining a report on the web, NTIS will offer a downloadable version. There is a nominal fee for each download for most publications.

For more information visit our website:

www.ntis.gov

U.S. DEPARTMENT OF COMMERCE
Technology Administration
National Technical Information Service
Springfield, VA 22161

FE-1790-4
Distribution Category UC-90c

ALLOY CATALYSTS WITH MONOLITH SUPPORTS FOR METHANATION OF COAL-DERIVED GASES

Phase 1

Annual Technical Progress Report
For Period April 22, 1975 to April 22, 1976

Calvin H. Bartholomew

Date Published--May 6, 1976

Under Contract No. E(49-18)-1790

PREPARED FOR THE UNITED STATES
ENERGY RESEARCH AND DEVELOPMENT ADMINISTRATION

Brigham Young University
Provo, Utah 84602

BIBLIOGRAPHIC DATA SHEET	1. Report No. FE-1790-4 (Annual)	2.	3. Recipient's Accession No.

4. Title and Subtitle
ALLOY CATALYSTS WITH MONOLITH SUPPORTS FOR METHANATION OF COAL-DERIVED GASES

5. Report Date
May 1976

6.

7. Author(s)
Calvin H. Bartholomew

8. Performing Organization Rept. No.

9. Performing Organization Name and Address
Catalysis Laboratory
Chemical Engineering Science
Brigham Young University
Provo, Utah 84602

10. Project/Task/Work Unit No.

11. Contract/Grant No.
E(49-18)-1790

12. Sponsoring Organization Name and Address
Energy Research and Development Administration
Fossil Energy ATTENTION: Dr. Paul Scott
20th Mass. Ave., N.W. Acting Assistant Director
Washington, D.C. 20545 University Programs

13. Type of Report & Period Covered
22 April 1975-22 April 76

14.

15. Supplementary Notes

16. Abstracts

This report details accomplishments during the first year of investigation of new pellet- and monolithic-supported alloy catalysts for methanation of coal synthesis gas. Hydrogen and carbon monoxide adsorption data were obtained for alumina-supported nickel, ruthenium, alloys of ruthenium with palladium and cobalt, and alloys of nickel with ruthenium, rhodium, molybdenum oxide, iron, cobalt, platinum, and palladium before and after exposure to low concentrations of hydrogen sulfide in hydrogen. Chemical analysis and x-ray diffraction measurements were made for selected samples. Design and construction of a high pressure laboratory reactor for catalyst testing was completed and all of the nickel containing catalysts were screened for methanation activity at 225 and 250°C and 1 atm. The principal investigator participated in six technical meetings and presented two papers in connection with this work.

17. Key Words and Document Analysis. 17a. Descriptors

Coal Gasification
Methanation
Catalyst(s)

17b. Identifiers/Open-Ended Terms

17c. COSATI Field/Group

PRICES SUBJECT TO CHANGE

18. Availability Statement	19. Security Class (This Report) UNCLASSIFIED	21. No. of Pages 89
	20. Security Class (This Page UNCLASSIFIED	22. Price $5.00-2.25

FOREWORD

This report summarizes technical progress during the first year (April 22, 1975 to April 22, 1976) of a two-year study conducted for the Energy Research and Development Administration (ERDA) under Contract No. E(49-18)-1790. The principal investigator for this work is Dr. Calvin H. Bartholomew; Dr. Paul Scott is the technical representative for ERDA.

The following students contributed to the technical accomplishments and to this report: Graduates - Blaine Barton, Don Stowell, and Richard Turner and Undergraduates - Norman Shipp, Richard Fowler and Scott Engstrom. Karen Weis and Scott Folster provided typing and drafting services. The assistance of Professor Charles Pitt (Department of Mining, Metallurgical and Fuels Engineering, University of Utah) in providing us with X-ray diffraction data is gratefully acknowledged.

TABLE OF CONTENTS

LIST OF TABLES

LIST OF TABLES (cont.)

LIST OF FIGURES

ABSTRACT

This report details accomplishments during the first year of investigation of new pellet- and monolithic-supported alloy catalysts for methanation of coal synthesis gas. Hydrogen and carbon monoxide adsorption data were obtained for alumina-supported nickel, ruthenium, alloys of ruthenium with palladium and cobalt, and alloys of nickel with ruthenium, rhodium, molybdenum oxide, iron, cobalt, platinum, and palladium before and after exposure to low concentrations of hydrogen sulfide in hydrogen. Chemical analysis and x-ray diffraction measurements were made for selected samples. Design and construction of a high pressure laboratory reactor for catalyst testing was completed and all of the nickel containing catalysts were screened for methanation activity at 225 and 250°C and 1 atm. The principal investigator participated in six technical meetings and presented two papers in connection with this work.

I. OBJECTIVES AND SCOPE

A. Background

Natural gas is a highly desirable fuel because of its high heating value and nonpolluting combustion products. In view of the expanding demand for and depletion of domestic supplies of clean fuels, economical production of synthetic natural gas (SNG) from coal ranks high on the list of national priorities.

Presently there are several gasification processes under development directed toward the production of methane or SNG. Although catalytic methanation of coal synthesis gas is an important cost item in the process, basic technological and design principles for this step are not well advanced. Extensive research and development are needed before the process can realize economical, reliable operation. Specifically, there appears to be important economical advantages in the development of more efficient, stable catalysts.

An extensive general review of the pertinent literature dealing with methanation catalysts was reported in the proposal, including reviews by Greyson(1) and Mills and Steffgen(2). From the literature, three major catalyst problems are apparent which relate to stability: (1) sulfur poisoning, (2) carbon deposition with associated plugging, and (3) sintering. These problems have received at best only modest attention. There has been very little research dealing with alloy catalysts for methanation, and there are no published investigations of the effects of catalyst support geometry on catalyst performance. This study deals specifically with sulfur poisoning, carbon deposition, and the effects of support (monolith and pellet) geometry on the performance of alloy methanation catalysts.

B. Objectives

The general objectives of this research program are (1) to study nickel and ruthenium alloy catalysts in the search for catalysts resistant to poisoning and carbon deposition and (2) to investigate the effects on catalytic efficiency of support (monolith and pellet) geometry. The work has been divided into five tasks to be completed over a period of two years:

Task 1. Prepare pellet- and monolithic-supported nickel and ruthenium alloy methanation catalysts by impregnation with metal salts of nickel, ruthenium, iron, platinum, etc. followed by reduction in hydrogen. Measure hydrogen and carbon monoxide chemisorption uptakes before and after exposure to hydrogen sulfide. Examine metallic phases of these catalysts by x-ray diffraction for chemical composition and particle size.

Task 2. Design and construct a continuous flow laboratory

reactor system capable of 25-1000°C and 1-25 atm. to be used for screening methanation catalysts and investigating effects of sulfur poisoning on methanation activity.

Task 3. Screen catalysts prepared in Task 1 using a reactor system constructed in Task 2 to determine methanation catalyst activity before and after exposure to 10 ppm H_2S.

Task 4. Compare the most promising catalysts based on the results of Tasks 1 and 3 for steady-state catalytic activity on different pellet and monolith supports of different hole sizes and geometries under various operating conditions, i.e., temperature, pressure, H_2/CO ratio and H_2S level.

Task 5. Maintain close liaison with organizations doing similar research such as the Bureau of Mines, Bituminous Coal Research, Institute of Gas Technology, and others.

C. Technical Approach

The technical approach which will be used to accomplish the tasks outlined above is presented in the revised proposal dated May 17, 1974. The main features of that approach are reviewed here along with more specific details and modifications which have evolved as a result of progress in related research over the past year. It is expected that various other aspects of this approach will be modified and improved as the project develops and as new data are made available. Nevertheless, the objectives, tasks and principle features of the approach will remain substantially the same.

Task 1: Catalyst preparation and characterization. Alumina pellets and extruded monolithic ceramic supports (provided by Corning Glass Works) coated with high surface area alumina will be impregnated with nickel nitrate and an alloying metal salt. Metals which will be alloyed with nickel include cobalt, iron, molybdenum, rhodium, ruthenium, platinum, and palladium. Ruthenium will be used in combination with nickel, cobalt and palladium. Approximately equimolar quantities of base metals will be used in combination with nickel. Only very small amounts of noble metal will be used in combination with nickel or other base metals. Catalyst samples will be dried in vacuum at 70-100° C, reduced at 500° C in flowing hydrogen, and carefully passivated with 1% air in preparation for further testing. A dedicated reduction apparatus will be used to reduce and passivate large batches of pellets and monolithic catalysts. Alloy catalysts will be initially prepared in pellet form for chemisorption, x-ray diffraction, and reactor screening measurements. Only the more promising catalysts will be prepared in monolithic form.

Hydrogen and carbon monoxide chemisorption uptakes will be measured using a conventional volumetric apparatus before and after exposure of each catalyst to hydrogen sulfide. Catalysts will be exposed to 10 ppm H_2S over a period of several hours in a dedicated

poisoning apparatus. X-ray diffraction measurements will be carried out to determine the active metallic phases and metal crystallite size where possible. Selected "aged" samples from Task 4 will be analyzed (by x-ray and perhaps ESCA) to determine carbon content and possible changes in phase composition or particle size. More extensive study of catalyst sintering or thermal degradation will be undertaken as part of a separate study supported by NSF and perhaps as an extension of this work, but is not intended to be within the scope of this two-year study.

Task 2: Laboratory reactor construction. It was initially proposed to construct a combination pulse-continuous flow reactor system for catalyst screening and testing. This apparatus was in fact constructed during the previous year as part of a previous methanation study supported by Corning Glass Works and Brigham Young University. The combination was found to be unworkable--unsatisfactory for pulse operation because of pulse broadening in the reactor and for continuous-flow operation due to high flow resistance in the small diameter tubing and sample valve. The reactor system was later modified for continuous-flow operation and collection of steady-state activity data, which were found to be more useful, realistic indicators of catalyst performance than the unsteady-state pulse measurements. Our continuous-flow reactor system, presently capable of 0-60 psig, will be modified for operation to 400 psig and significantly upgraded to enable convenient study of activity as a function of temperature, pressure, and feed composition.

Task 3: Reactor screening of alloy catalysts. Catalyst samples will be screened on the basis of steady-state methanation activity (reaction rate based upon catalyst surface area) measured in a differential flow reactor at atmospheric pressure and 225 or 250°C at a fixed H_2/CO ratio of 3.5-4.0. Samples to be screened will include freshly-reduced catalysts and catalyst samples exposed in a separate poisoning system to 10 ppm H_2S over a period of 6-18 hours.

Task 4: Catalyst geometry testing and design. The most promising catalysts based on the results of screening will be tested for activity and conversion as a function of pressure, temperature, H_2/CO ratio, and H_2S concentration. The conversion of carbon monoxide to methane as a function of temperature will be determined for various pellet and monolith geometries at both high and low pressures. The effects of water addition to the feed stream will also be investigated. Conversion of carbon monoxide to methane during *in situ* exposure to low levels of hydrogen sulfide and at low H_2/CO ratios will be used as a measure of stability toward sulfur poisoning and carbon deposition. A comparison of steady-state conversions at given temperature and pressure conditions for monolithic supports of different hole sizes and geometries will be used to optimize the geometry of the catalyst support.

Task 5: Technical visits and communication. Visits to other methanation laboratories such as the Pittsburgh Energy Research Center and the Institute of Gas Technology are planned. Close communication

with other researchers working in methanation catalysis both in industrial and academic locations is also planned. The principal investigator will attend coal and catalysis meetings regularly to communicate with other workers regarding methanation catalysis.

II. SUMMARY OF PROGRESS

A project summary is presented in Figure 1 and accomplishments during the past year are summarized below. Figure 1 shows that task accomplishments are either on or ahead of schedule.

Accomplishments during the past year are best summarized according to task:

Task 1. A catalyst reduction system, a poisoning apparatus, and a new chemisorption-vacuum system were designed, constructed, and tested. Alumina-supported Ni, Ni-Ru, Ni-Rh, MoO_3, Ni-MoO_3, Ni-Fe, Ni-Co, Ni-Pt, Ni-Pd, Ni-Cu, Ru-Pd, Ru-Pt, and Ru-Co catalysts were prepared in pellet form by impregnation, drying and reduction in hydrogen. Several monolithic-supported Ni-Al_2O_3 catalysts were prepared by special impregnation techniques followed by drying and reduction. Hydrogen and carbon monoxide adsorption uptakes were measured for all of the pellet-supported catalysts (except Ni-Cu and Ru-Pt) before and after exposure to 10 and/or 25 ppm H_2S in hydrogen. Hydrogen adsorption uptakes were measured for monolithic-supported nickel catalysts. Methods for measuring CO adsorption on nickel were tested extensively using a pure unsupported nickel powder and a 3% Ni/Al_2O_3. The procedures for poisoning catalysts with H_2S were refined and the concentration of H_2S/H_2 was determined analytically. Chemical analysis was performed for several Ni/Al_2O_3 catalysts and X-ray fluoresence measurements to perform routine chemical analysis were initiated. X-ray diffraction measurements were obtained for three Ni/Al_2O_3 catalysts and alumina-supported Ni-Fe, Ni-Co, Ru-Co, Ni-Pt, and Ni-Pd catalysts to determine phase composition and particle size.

Task 2. An atmospheric pressure laboratory reactor used for catalyst testing was redesigned to (1) allow for operation to 400 psia (2) enable more efficient, reproducible operation by addition of mass flowmeters, a better furnace with temperature programming, etc. and (3) improve the accuracy of gas phase analysis by addition of infrared analysis for CO and chromatographic accessories. The associated equipment and supplies for the new system were ordered, installed, and tested. System upgrading was essentially completed. A dilution-calibration apparatus was designed, built, and used in preparation of gas calibration standards.

Task 3. Catalyst screening and testing procedures were designed and refined to give rapid, useful comparisons of methanation activity under steady state conditions. In addition, procedures for data collection and reduction were designed and tested. Screening measurements of steady state activity at 225, 250, and 275°C and 1 atm were carried out for alumina-supported Ni, Ni-Ru, and Ni-Rh catalysts. In addition, screening measurements of steady-state methanation activity at 225, 250°C and space velocities of 30,000 and 60,000 hr^{-1} (also 1 atm) were carried out for alumina-supported Ni, Ni-Ru, Ni-Rh, Ni-Pt, Ni-Pd, Ni-Fe, Ni-Co, Ni- MoO_3, Ni-Cu, and Ru-Pt catalysts. Conversion

Task No.	Work Statement
1. a.	Catalyst Preparation
b.	Catalyst Characterization
2.	Lab Reactor Construction
3.	Catalyst Screening
4.	Catalyst Testing and Design
5.	Visits and Technical Communication

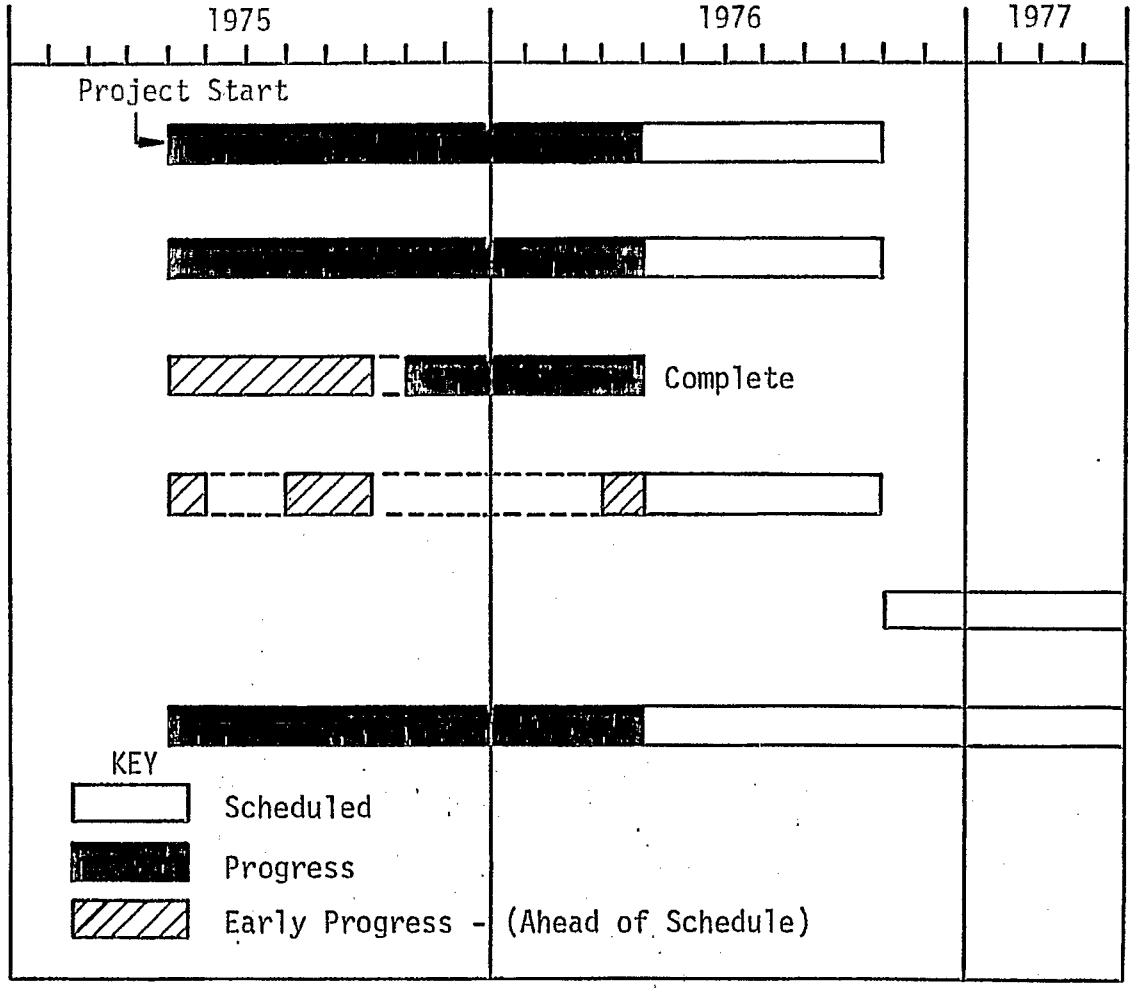

Figure 1. Project Progress Summary

as a function of temperature and the effect of passivation on activity were studied on a 15 wt.% Ni/Al_2O_3 catalyst. Conversion as a function of temperature was also measured for a commercial (G-87) catalyst and the results were compared with those for the 15 wt.% Ni/Al_2O_3.

Task 4. Work is scheduled to begin October 22, 1976.

Task 5. The principal investigator has established technical communications with other workers in methanation catalysis. He attended the Symposium on Catalytic Conversion of Coal held April 21-23, 1975 in Pittsburgh, participated in the University Contractors' Conference (sponsored by ERDA/ EPRI/NSF-RANN) held October 22-23 in Park City, Utah, attended the California Catalysis Society Meeting (Nov. 7-8), presented a paper at the 68th annual AIChE meeting in Los Angeles (Nov. 16-22), attended a short course on Catalysis Deactivation (Nov. 17-18), chaired the First Rocky Mountain Fuel Symposium held January 30, 1976 at BYU, and attended the Spring Meeting of the California Catalysis Society held March 25-26 in Berkeley. Mr. Kyung Sup Chung also attended the University Contractors' Conference and Mr. Blaine Barton presented a paper at the Rocky Mountain Fuel Symposium. The principal investigator has finalized plans to visit other methanation laboratories during the next quarter.

Miscellaneous. Mr. Kyung Sup Chung completed his master's thesis dealing with "The Effects of H_2S Poisoning on H_2 and CO Chemisorption on Nickel and Nickel Alloys."

III. DETAILED DESCRIPTION OF TECHNICAL PROGRESS

A. Task 1: Catalyst Preparation and Characterization

1. Catalyst preparation. Alumina pellet-supported nickel and ruthenium alloy catalysts were prepared according to the general procedure oulined in Table 1. Table 2 is a list of catalysts prepared with codes, amounts, compositions and preparation techniques. Kaiser SAS 5 x 8 mesh alumina (301 m^2/g) calcined at 600°C for 2 hours was used in all of the preparations. Further details of preparation for each catalyst can be found in earlier quarterly reports (3-5). Several monolithic-supported nickel catalysts were prepared using a variety of techniques in order to find the most efficient preparation; compositions and preparation techniques are summarized in Table 3.

2. Hydrogen and Carbon Monoxide Chemisorption on Nickel and Nickel Alloys and Effects of Hydrogen Sulfide on Adsorption.

a. Equipment and materials. Gas adsorption measurements were carried out in a conventional Pyrex glass volumetric adsorption apparatus (see Fig. 2) capable of 10^{-6} Torr vacuum, which consisted of an oil diffusion pump and a rotary mechanical pump isolated from the adsorption system by a liquid-nitrogen cooled trap. The pressure was measured with a Granville-Phillips ionization gauge. Each catalyst sample was placed in a Pyrex flow-through cell to enable reduction of samples in flowing hydrogen prior to the chemisorption measurement. The amount of gas adsorbed by the catalyst was determined by means of a calibrated gas buret connected to a manometer backed with a metrically-calibrated mirror (see Fig. 2). A similar vacuum adsorption apparatus with Bourdon tube (Texas Instrument) pressure measurement was designed, constructed and used in this study. The details of design and construction for this apparatus and a large reduction apparatus were presented in an earlier report (3).

In principle it is possible to use either of the chemisorption-vacuum systems for controlled, in situ exposure of catalyst samples to H_2S. However, in practice, there were difficulties encountered with contamination of the system, adsorption in the molecular sieve trap, and significant variations in the flow of the H_2S/H_2 stream. To avoid these difficulties a separate poisoning apparatus was constructed according to the design sketched in Figure 3. The H_2S concentration was determined analytically using a technique described earlier (5).

b. Catalyst pretreatment and procedure. All catalyst samples were prepared in accordance with the general scheme shown in Table 1. Most of the samples used in adsorption measurements were reduced in situ using a glass cell of the design shown in Figure 3. Samples pre-reduced and passivated in a large quartz tube were again reduced in flowing hydrogen for a minimum of 2 hours at 450°C prior to adsorption

TABLE 1

General Catalyst Preparation Scheme

Step	Procedure
Drying	Samples are dried: 1. In a forced-circulating-air oven at 80-100°C for 24 hours. 2. In a vacuum oven, 100-115°C for 12-24 hours.
Reduction	Sample is purged in flowing N_2 or evacuated to 5×10^{-4} Torr at 120-150°C. Reduction in flowing hydrogen (700-2000 GHSV) is according to the following temperature schedule: • 0-230°C at less than 5°C/min • 230°C hold for 1 hour • 230-450°C or 230-500°C at less than 5°C/min • 450-500°C hold for 10-16 hours
Passivation	Sample is exposed to a stream or doses of less than 1% air in nitrogen or helium over a period of 15 to 20 minutes. The concentration of air is then gradually increased to 100%.

TABLE 2

Preparation of Alumina-Supported
Nickel and Nickel-Alloy Catalysts

Catalyst	Code	Amount	Composition (wt.%)	Preparation
Ni/Al_2O_3	Ni-A-111	500g	3.0% Ni	2 impregnations
$Ni-Ru/Al_2O_3$	Ni-Ru-A-100	20g	2.5% Ni .5% Ru	acidic 1 impreg.
$Ni-Ru/Al_2O_3$	Ni-Ru-A-101	20g	2.5% Ni .5% Ru	ion exchange
$Ni-Ru/Al_2O_3$	Ni-Ru-A-102	20g	2.5% Ni .5% Ru	basic 2 impreg.
$Ni-Ru/Al_2O_3$	Ni-Ru-A-103	20g	2.5% Ni .5% Ru	Same as Ni-Ru-A-100
$Ni-Ru/Al_2O_3$	Ni-Ru-A-104	150g	2.5% Ni .5% Ru	acidic 1 impreg.
$Ni-Ru/Al_2O_3$	Ni-Ru-A-105	150g	2.5% Ni .5% Ru	basic 2 impreg.
$Ni-Ru/La/Al_2O_3$	Ni-Ru-La-A-100	20g	2.5% Ni .5% Ru 3.0% La	basic 2 impreg.
$Ni-Ru/La/Al_2O_3$	Ni-Ru-La-A-101	20g	2.5% Ni .5% Ru 3.0% La	acidic 1 impreg.
$Ni-Rh/Al_2O_3$	Ni-Rh-A-100	70g	2.5% Ni .5% Rh	acidic 2 impreg.
$Ni-MoO_3/Al_2O_3$	$Ni-MoO_3$-A-101	200g	2.5% Ni 3.0% MoO_3	basic 5 impreg.
$Ni-Fe/Al_2O_3$	Ni-Fe-A-100	100g	10% Ni 10% Fe	acidic 3 impreg.
$Ni-Co/Al_2O_3$	Ni-Co-A-100	100g	10% Ni 10% Co	neutral 2 impreg.

TABLE 2 continued

Catalyst	Code	Amount	Composition (wt.%)	Preparation
$Ni-Pt/Al_2O_3$	Ni-Pt-A-100	100g	15% Ni 0.5% Pt	slightly acidic 2 impreg.
$Ni-Pd/Al_2O_3$	Ni-Pd-A-100	100g	15% Ni 1% Pd	acidic 2 impreg.
$Ni-Cu/Al_2O_3$	Ni-Cu-A-100	100g	5% Ni 0.6% Cu	neutral solution of nitrates 2 impreg.
MoO_3/Al_2O_3	MoO_3-A-100	100g	3% MoO_3	$(NH_4)_6Mo_7O_{24}$ $\cdot 4H_2O$ dissolved in ammonical solution
$Ru-Co/Al_2O_3$	Ru-Co-A-100	100g	0.52% Ru 15.0% Co	acidic
$Ru-Pd/Al_2O_3$	Ru-Pd-A-100	100g	0.49% Ru 0.51% Pd	acidic
$Ru-Pt/Al_2O_3$	Ru-Pt-A-100	80g	0.5% Ru 0.5% Pt	$RuCl_3$ and $H_2PtCl_6 \cdot 9H_2O$ 2 impreg.
Ni/Al_2O_3	Ni-A-112	500g	3% Ni	2 impregnations

TABLE 3

Nominal Composition and Hydrogen Chemisorptive Uptake Data for Monolithic-Supported Nickel Catalysts

Catalyst	Nominal Composition	Preparation*	H_2 Uptake (μmoles/g-catalyst)	% Dispersion	Surface Area (m^2/g-cat.)
Ni-M-101	15.7 wt% Ni 13.5 wt% Al_2O_3	Nickel nitrate melt (6) Washcoat - Dispal Al_2O_3 slurry (8)	45.2	3.38	3.69
Ni-M-103	13.7 wt% Ni	Nickel - Aqueous nickel soln., ppt. with NH_3 (11)	96.5	8.27	7.87
	13.2 wt% Al_2O_3	Washcoat - SA Medium Al_2O_3 slurry (3)			
Ni-M-104	15.9 wt% Ni	Nickel nitrate melt (3)	97.6	7.21	7.96
	19.9 wt% $NiAl_2O_3$	Washcoat - SA Medium Al_2O_3 slurry plus Ni Nitrate to form $NiAl_2O_4$ (6)			
Ni-M-105	16 wt% Ni	Nickel - Aqueous nickel soln. (15)	70.2	5.15	5.72
	12.6 wt% $NiAl_2O_4$	Washcoat - Ni & Al Nitrate slurry to give $NiAl_2O_4$ (8)			
Ni-M-106	18.5 wt% Ni 14.1 wt% Al_2O_3	Nickel - Aqueous nickel soln. (5) Washcoat - SA Medium Al_2O_3 slurry (3)	83.3	5.29	6.79
Ni-A-116	15 wt% Ni	Alumina Pellets	187.8	14.7	15.39

* the number of metal applications or support washcoats is given in parentheses

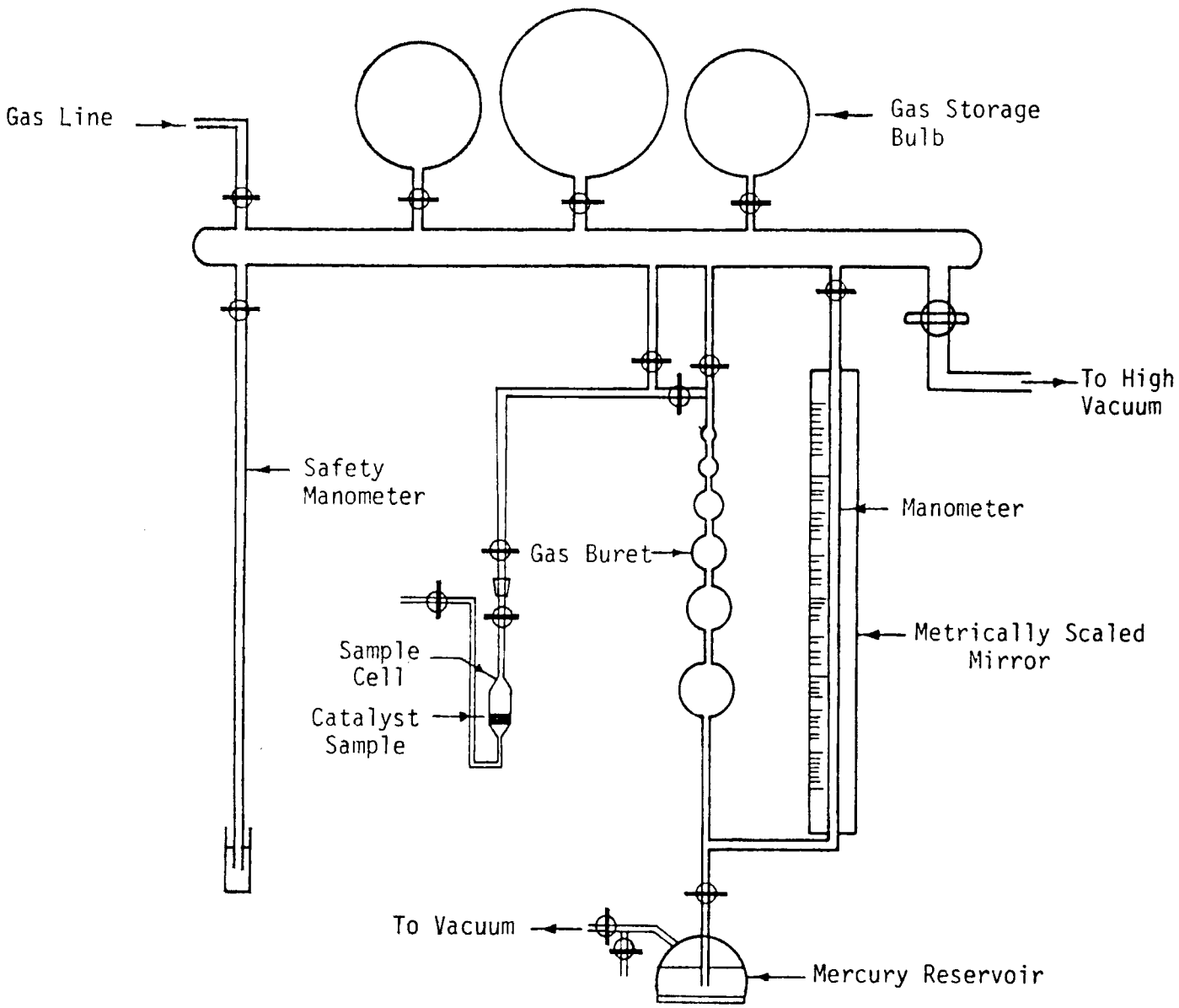

Figure 2. Volumetric Chemisorption Apparatus

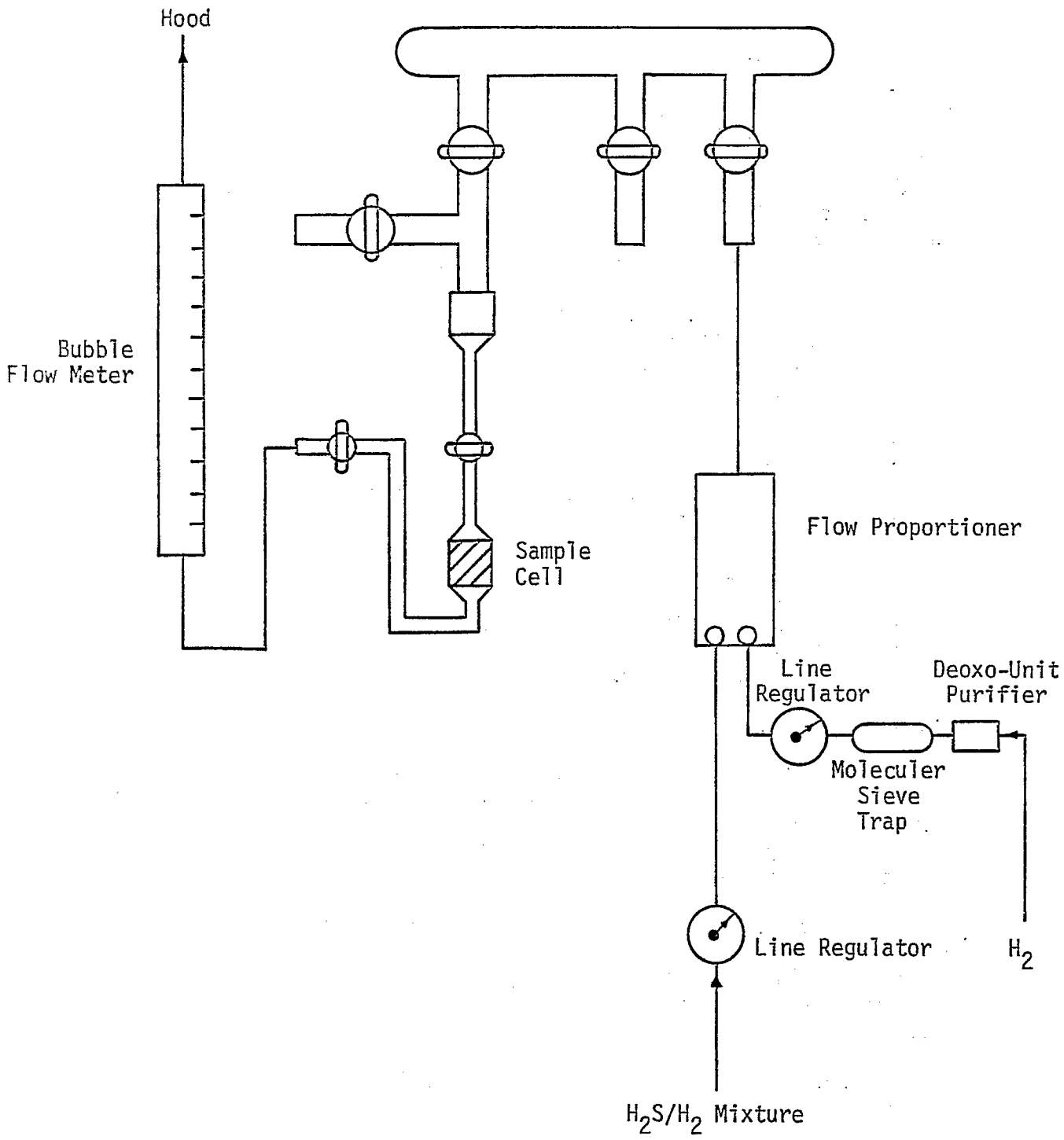

Figure 3. Poisoning Apparatus

measurements. Ni-Fe/Al_2O_3 samples were found to require at least 6 hours reduction at 450°C for complete reduction after exposure to air.

The standard procedure used in measuring hydrogen adsorption uptake is presented in Table 4 and is based upon surveys of the literature (6) and upon adsorption studies (3-5, 7, 8) of nickel catalysts over the past two years. A similar procedure was used for ruthenium catalysts except that a longer equilibration time (about 2 hours) was necessary. This procedure was only modified slightly for monolithic samples in that a longer evacuation period was necessary because of the large surface area per sample. In the case of Pd containing samples, the adsorption measurements were carried out at 100°C to prevent interferring absorption.

Catalyst surface area and dispersion were calculated (3) using hydrogen uptake data and assuming (1) the number of hydrogen atom/surface metal atom = 1, (2) complete reduction of nickel and nickel alloys to the metallic state (except for Ni-MoO_3), (3) a surface metal composition identical to the bulk metal composition, and (4) planar site densities (see Appendix) based upon the three lowest index crystallographic planes for each metal. Assumptions 1-3 are currently under investigation as part of the NSF methanation study in this laboratory.

The measurement of carbon monoxide adsorption uptake for nickel and nickel alloy catalysts was carried out according to a procedure shown in Table 5. Unfortunately, the uptake data for a given sample were found to vary greatly according to various changes in procedure such as modifications in the equilibration pressure and temperature. In fact, the ratio of adsorbed carbon monoxide atoms to hydrogen atoms varied from 0.5 to 4.7 depending upon modifications in procedure. Moreover, there is apparently formation of nickel carbonyl at 25°C which further complicates the measurements. Thus, carbon monoxide adsorption measurements were carried out at -85°C and relatively high equilibration pressures (400-500 Torr). Unfortunately, under these conditions there is also considerable physical adsorption on the support.

Controlled poisoning of catalysts by H_2S involved 6 or 12 hour exposure of small samples to a flowing stream of 10, 25 or 50 ppm H_2S in H_2 at 450°C using the apparatus sketched in Figure 3. Details of calibration and operation have been described in QPR-3 (5).

The basic steps in pretreatment and surface area measurement are as follows:

1. A large sample (50-100g) consisting of Al_2O_3 pellets impregnated with metal salts is dried at 100°C and reduced at 450-500°C at a hydrogen space velocity of 1500 hr^{-1}.

2. H_2 chemisorptive uptake is measured for a small sample

TABLE 4

Standard Procedure for Measuring H_2 Uptake of Nickel Catalysts

Step	Procedure
Reduction	Reduce in situ - 10-16 hrs. at 450-500°C Reduce previously reduced catalysts - 2 hrs. at 450°C
Evacuation	Evacuate - 1-2 hrs. at 400-450°C and usually to about 10^{-5} Torr
Adsorption	1. Expose evacuated sample to measured amount of hydrogen at 25°C and 400-500 Torr for 45 minutes (200 minutes for ruthenium containing catalysts) 2. Measure moles of hydrogen as a function of pressure from 0-400 Torr
Calculation	Plot hydrogen uptake versus pressure and extrapolate to zero pressure to determine uptake due to chemisorption

TABLE 5

Procedure for Measuring CO Uptake
of Nickel Catalysts

Step	Procedure
Reduction (in H_2)	Reduce in situ - 10-16 hours at 450-500°C Reduce previously reduced catalysts - 2 hrs. at 450°C
Evacuation 1	Evacuate - 1-2 hrs. at 400-500°C and usually to about 10^{-5} Torr
Adsorption 1	1. Expose evacuated sample to measured amount of CO at -83° and 400-500 Torr for 30-60 min. 2. Measure moles of CO as a function of pressure from 0-400 Torr
Evacuation 2	Evacuate 30-60 min. at -83° and usually to 10^{-3} to 10^{-4} Torr
Adsorption 2	1. Expose sample to measured amount of CO at -83° and 400-500 Torr for 30-60 min. 2. Measure moles of CO as a function of pressure from 0-400 Torr
Calculations	Plot both isotherms (moles uptake versus pressure). Correct the first isotherm for chemisorption on the support. Determine the difference between isotherms at zero pressure which corresponds to amount chemisorbed on the metal.

(2-3g) at 25°C (135°C for Pd or Ru samples) and CO uptake at -83°C.

3. The sample is exposed to 10 or 25 ppm H_2S at 450°C for 6 hours (GHSV = 2000 hr^{-1}).

4. H_2 and CO uptakes are again measured.

5. The sample is exposed to 10 ppm H_2S at 450°C for an additional 6 hours.

6. H_2 and CO uptake measurements are repeated.

Throughout the entire procedure the sample is contained in the same glass sample cell to prevent exposure to the atmosphere.

c. Adsorption data. Hydrogen uptake, percent dispersion, and surface area data are listed in Table 6 for nickel, nickel alloy and ruthenium alloy catalysts prepared in this study. A typical hydrogen adsorption isotherm is shown in Figure 4 for 3% Ni/Al_2O_3. Hydrogen adsorption isotherms were shown in earlier reports (3-5) for each of these catalysts. Hydrogen adsorption uptakes were determined by extrapolating to zero the straightline portion of each isotherm above the saturation pressure (about 100 Torr). The relatively small values for the slopes of these isotherms indicate that physical adsorption on the support is a small effect at 25°C.

One of the objectives of this study is to find catalysts for methanation which are more efficient, active, and stable than nickel. One measure of efficiency is the active catalyst surface area per unit mass or volume. The magnitude of the hydrogen uptake in moles/gram of catalyst depends upon (1) the amount of active metal(s) in the sample and (2) the dispersion (or particle size) of the active component(s). Previous work (7) in this laboratory has established that metal dispersion decreases with increased nickel loading in the nickel-alumina system. This same effect is also apparent in the data for 3, 15 and 32 wt.% Ni in Table 6; in fact, the 15 wt.% Ni catalyst prepared in this laboratory has a higher surface area and significantly higher dispersion than the 32 wt.% commercial nickel (Girdler G-87). This can be explained in terms of differences in preparation and pretreatment. Commercial catalysts are normally prepared by calcination of the impregnated or precipitated supported metal salt followed by reduction in hydrogen. This high temperature calcination ultimately prevents complete reduction of nickel to the metallic state; in fact, a typical commercial nickel probably contains 30-50% NiO and/or $NiAl_2O_4$ even after reduction in flowing hydrogen at 500°C (7). Our catalysts on the other hand are prepared by direct reduction of the supported metal salt in hydrogen to produce samples containing 80-90% of the metal in the metallic state and in a significantly higher state of dispersion compared to calcined samples (7).

TABLE 6

Hydrogen Chemisorptive Uptake Data for Alumina-Supported Nickel Nickel Alloy and Ruthenium Alloy Catalysts

Catalyst	Nominal Composition (wt%)	H_2 Uptake (μmoles/gram)	Metal Particle Size (A)	Percent Dispersion	Surface Area (m^2/g)
Ni-A-111	3% Ni	21.4	116	8.35	1.75
Ni-A-112	3% Ni	39.4	63	15.4	3.23
Ni-A-116	14% Ni	187.8	62	15.7	15.39
G-87 (Girdler)	32% Ni	161.6	163	5.93	13.24
Ni-MoO_3-A-101	2.5% Ni - 3% MoO_3	22.5	92*	10.6*	1.84*
MoO_3-A-101	3% MoO_3	1.0	--	--	--
Ni-Ru-A-105	2.5% Ni - 0.5 wt% Ru	44.6	52	18.76	3.71
Ni-Rh-A-100	2.5% Ni - 0.5% Rh	38.3	62	16.1	3.16
Ni-Co-A-100	10% Ni - 10% Co	114.9	142	6.76	9.54
Ni-Fe-A-100	10% Ni - 10% Fe	80.6	278	4.60	5.14
Ni-Pt-A-100	15.7% Ni - 0.5% Pt	106	119	8.22	8.66
Ni-Pd-A-100	15% Ni - 1.0% Pd	107.4	115	8.13	8.82
Ru-Pd-A-100	0.49% Ru - 0.51% Pd	21.0	24	43.6	2.08
Ru-Co-A-100	0.52% Ru - 15% Co	48.3	253	3.72	4.11

* Based upon nickel only

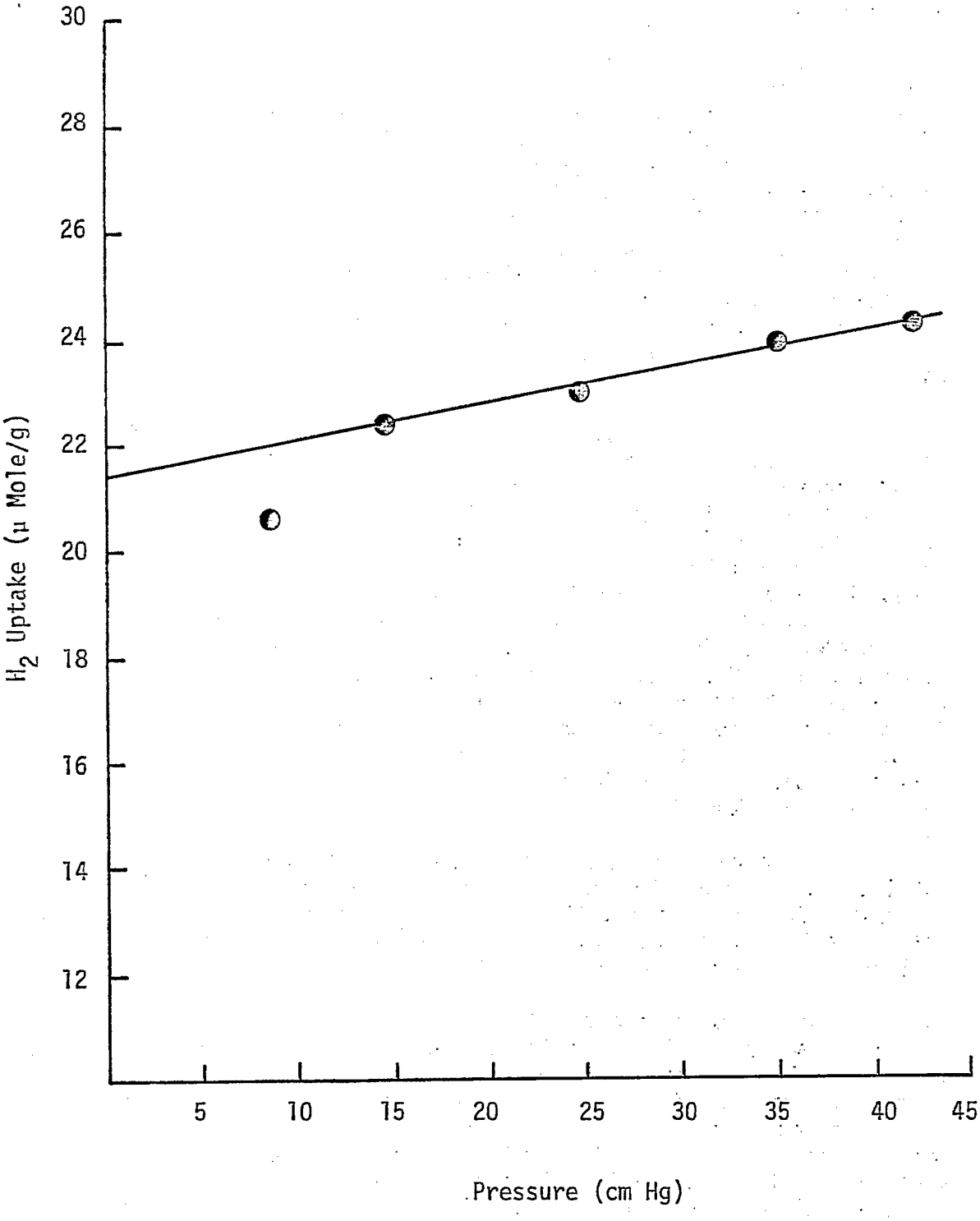

Figure 4. H_2 Chemisorption on Ni-A-111 at 25°C.

Comparison of surface areas and dispersions from Table 6 for nickel alloys compared to nickel catalysts show approximately the same surface areas for 3% Ni-Rh and 3% Ni-Ru compared to the 3% Ni catalyst. The 5.5% Ni-Mo catalyst, however, has approximately half the surface area of the 3% Ni, possibly because of interaction of part of the nickel with MoO_3 to form a complex which does not adsorb hydrogen. Moreover, the data for the 3% MoO_3/Al_2O_3 indicate that hydrogen adsorption on the molybdenum oxide is negligibly small. These observations suggest that the nickel sites do and the MoO_3 sites do not chemisorb hydrogen. All of the alloys in the 15-20% range have 40-50% lower surface areas compared to the 15% Ni/Al_2O_3. The dispersion of Ru-Co is the lowest, Ru-Pd the highest. In regard to the effects of alloy composition on CO and H_2 chemisorption, it is, in principle, possible that actual chemisorptive uptakes for alloys would be mole weighted averages of the individual metallic constituent uptakes; however, in practice this does not necessarily hold, and it is more likely that the surface compositions are not the same as the bulk compositions for many of these alloy catalysts (9).

Hydrogen adsorption uptakes, nickel dispersions and surface areas are shown for monolithic supported nickel catalysts in Table 3. A comparison of the hydrogen uptake data shows Ni-M-103 and Ni-M-104 to have the highest uptakes, Ni-M-103 has the highest dispersion, while the Ni-M-104 catalyst, by virtue of its higher loading, has the highest surface area. Though these two catalysts are nearly equal in terms of uptake data, the Ni-M-104 catalyst requires far fewer impregnations to reach a reasonable nickel loading. This may be considered a significant advantage, as each impregnation requires several hours of additional preparation time. Ni-M-106 also requires few impregnations and has an uptake nearly as great as that of Ni-M-104. Therefore, the techniques used to prepare Ni-M-104 and Ni-M-106 (or some combination of these techniques) appear to be the most promising methods of monolithic-supported catalyst preparation thus far investigated.

A comparison of the dispersions of the monolithic-supported catalysts with that of Ni-A-116 shows that the monoliths have roughly one-half the dispersion. This is to be expected as the monolithic catalysts have approximately a 50% loading of nickel on the alumina coating, as compared to 15% for Ni-A-116 (7).

Table 7 summarizes data for chemisorption of CO on nickel, nickel alloys and ruthenium alloys. Figures 5 and 6 are representative isotherms for unsupported and supported nickel. The data in Table 7 show the ratios of adsorbed carbon monoxide molecules to hydrogen atoms ranging from 0.61 to as high as 3.54. The higher ratios indicate the possibility of multiple adsorption of CO molecules on metal atoms (i.e. formation of surface metal carbonyls), and the results are generally in agreement with previous studies of nickel, ruthenium, and rhodium catalysts. Any large discrepancies between our CO adsorption data and those reported by others are very likely due to differences in equilibration pressure. Data from an earlier report (3), for

TABLE 7

CO Chemisorption Uptakes for Alumina-Supported Nickel and Ruthenium Catalysts

Catalyst	Nominal (wt%) Composition	H_2 Uptake (μmole/g)	CO Uptake (μmoles/g)	CO/H
Kaiser Al_2O_3	Pure Al_2O_3	0.5	26.3	26.3
Inco Ni Powder	Pure Ni	3.47	5.3	0.76
Ni-A-111	3% Ni/Al_2O_3	21.4	80.0	1.87
Ni-MoO_3-A-101	2.5% Ni. 3% MoO_3	24.0	107.3	2.23
MoO_3-A-101	3% MoO_3	1.0	8.0	4.0
Engelhard Ru	0.5% Ru	7.62	54.0	3.54
Ni-Ru-A-105	2.5% Ni 0.5% Ru	47.6	148.2	1.56
Ni-Rh-A-100	2.5% Ni 0.5% Rh	43.5	145.6	1.67
Ni-Fe-A-100	10% Ni 10% Fe	80.6 118.0	259.0 274.8	1.61 1.16
Ni-Co-A-100	10% Ni 10% Co	114.9 116.0	173.8 190.8	0.76 0.82
Ni-Pd-A-100	15% Ni 1% Pd	107.4 75	145.5 175.5	0.68 1.17
Ni-Pt-A-100	15.7% Ni 0.5% Pt	106.0 107.5	206.0 363	0.97 0.66
Ru-Pd-A-100	0.49% Ru 0.51% Pd	21.0	70.0	1.67
Ru-Co-A-100	0.52% Ru 15% Co	48.3 40.4	58.5 69	0.61 1.30

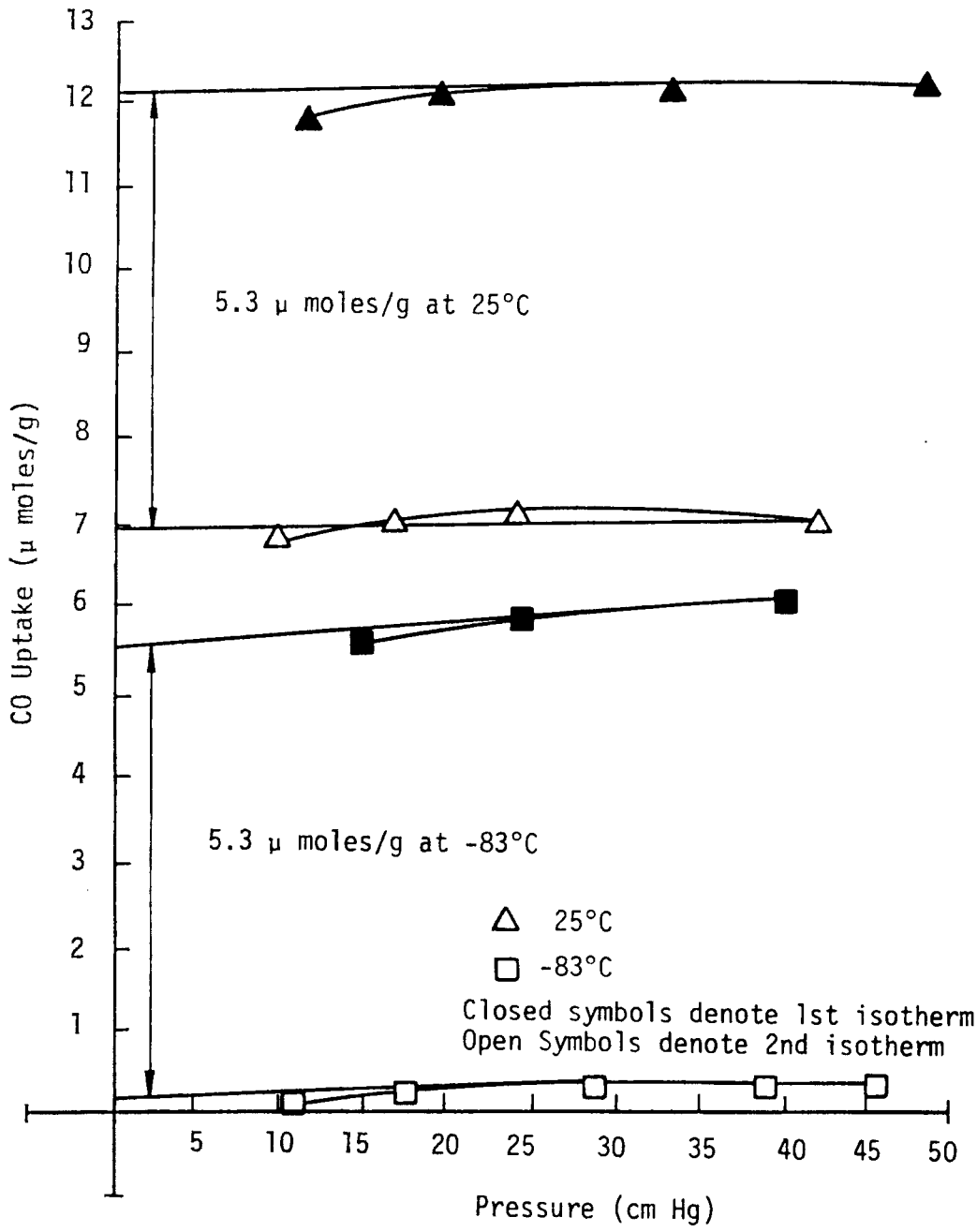

Figure 5. CO Adsorption on Inco Nickel Powder at 25° and -83°C.

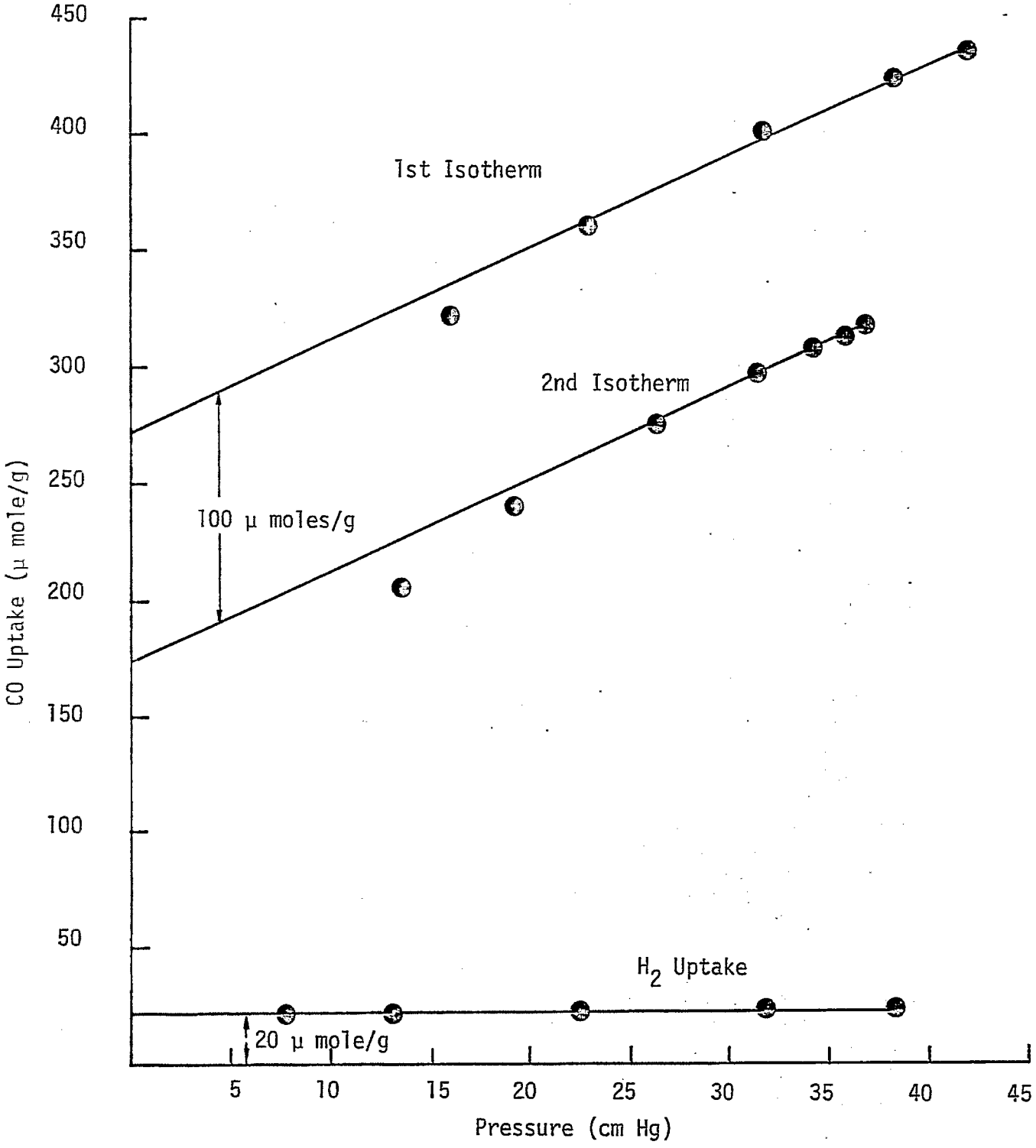

Figure 6. CO Chemisorption on Ni-A-111 at -83°C

a nickel catalyst show that CO uptake can vary significantly as a function of equilibration pressure; in other words the monolayer coverage of CO is not well defined. Moreover, there is evidence from the literature and from our data which suggests that metal carbonyl formation occurs at the surface during exposure to CO for many catalyst systems. A detailed discussion of most of these results and comparison with the literature was presented in an earlier report (4), the most important aspects of which will be summarized here. New data for the last four catalysts in Table 7 are also discussed below.

Data from Table 7 for Kaiser SAS Al_2O_3 show that CO uptake is significant at 25 and -83°C. These support uptake data were used to correct for chemisorption on the support in determining CO uptake for the alumina-supported catalysts listed in Table 7.

Isotherms for CO adsorption on an Inco nickel powder (a high purity nickel having particles in the 1-3 micron range) are shown in Figure 5. The first isotherm at 25°C corresponds to the CO uptake of the sample obtained after evacuation at 400°C; the CO adsorption extrapolated to zero pressure is 12.1 micromoles/g of nickel and corresponds to a value of CO/H of 1.74. Recent nitrogen and argon BET and H_2 chemisorption measurements (8) (this laboratory) for the same nickel powder and previous data by O'Neill (10) using argon BET and H_2 chemisorption on a nickel powder show that hydrogen chemisorbs dissociatively on nickel with a surface stoichiometry of $H/Ni_s = 1$. These H_2 and CO chemisorption data together provide strong evidence for the existence at 25°C of surface complexes such as $Ni(CO)_2$ and $Ni(CO)_3$.

After evacuation of the CO covered nickel powder at 25°C, the second isotherm (at 25°C) was obtained--the amount corresponding to carbon monoxide (or possibly nickel carbonyl) removed by evacuation at room temperature. The difference between the first and second isotherm, 5.3 moles/g corresponds to irreversibly held CO, and the corresponding CO/H value is 0.76. CO uptake data for the Inco nickel powder at -83°C show the same amount of irreversibly adsorbed CO as compared to 25°C but a negligible uptake for the second isotherm. In other words, at -83°C the initial CO/H value is 0.76 and there is no reversibly adsorbed CO (or nickel carbonyl) which can be pumped off at -83°C.

In summary, our data for the nickel powder combined with earlier observations (3) of nickel loss for Ni/Al_2O_3 samples strongly suggest nickel carbonyl formation at 25°C whereas at -85°C no easily evacuated carbonyl is formed. Hence, our procedure involving CO adsorption at -83°C avoids the problem of carbonyl formation and loss of nickel metal or alternatively loss of reversibly adsorbed CO.

The data in Table 7 for 3% Ni/Al_2O_3 show a value of CO/H of 1.87 suggesting that twice as many CO molecules are adsorbed on the nickel catalyst as hydrogen atoms. Recent studies in our

laboratory (7) have shown that in alumina-supported nickel catalysts prepared according to our techniques, almost 90% of the surface nickel is reduced to nickel metal; unreduced nickel is presumably NiO. Since measurements in our laboratory indicate negligible CO adsorption on NiO, our CO chemisorption results suggest that either CO/ Ni_s = 2 or that there is CO "spillover" from the nickel crystallites on to the support.

The data in Table 7 show that nickel in combination with ruthenium or rhodium adsorbs about twice as many CO molecules as hydrogen atoms. This is not unexpected since the separate metals behave very similarly and are also observed to form carbonyls. On the other hand, cobalt combined with either nickel or ruthenium adsorbs less carbon monoxide molecules per site then do nickel or ruthenium. Pt and Pd exert a similar strong influence on the adsorption behavior by significantly lowering the CO/H ratio, even though these metals are only present in the samples in the amount of 1 and 3.6 at % respectively. Alday, et al. (11) and Scholten (12) have reported that CO/H ratios for Pd vary from about 0.39 to 1.1 depending upon temperature and crystallite size. Our data also show effects of crystallite size. For example, in the case of Ni-Pd-A-100 the ratio increased from 0.68 to 1.17 as the particle size increased from 115 to 164 A. The increase in CO/H with increasing crystallite size observed in our experiments, however, shows a trend which is opposite to that observed in other studies. For Pt, several authors (13-15) report CO/H values varying from 0.3 to 1. Thus, the low CO/H values observed for Ni-Pd and Ni-Pt are consistent with those observed for the noble metals suggesting the possibility that Pd and Pt may be concentrated at the alloy surface.

d. Effects of H_2S on CO and H_2 adsorption. Table 8 summarizes data obtained for several catalysts during the first 3 quarters showing changes in H_2 and CO adsorption after exposure to 10 ppm H_2S for 6 and 12 hours. Figures 7 and 8 are representative isotherms illustrating the effects of H_2S on H_2 and CO adsorption for two of the samples described in Table 8. Two very significant trends are apparent from the data in Table 8. First the effect of H_2S exposure is to decrease the H_2 uptake of the sample; second CO chemisorption is generally increased (except for the ruthenium catalyst). The increase in CO adsorption after H_2S exposure is a most surprising result! A detailed discussion of these results was presented in QPR-2 (4) and QPR-3(5). The decrease in hydrogen adsorption after H_2S exposure is believed to be due to blocking of adsorption sites by adsorbed sulfur. The increase in CO adsorption may be due to formation of a surface complex such as $(CO)_xS$. An alternative or possibly contributing mechanism is that of carbon monoxide or COS spillover from the metal surface to the support.

During the last quarter, poisoning studies for Ni-Pt-A-100, Ru-Co-A-100, Ni-Pd-A-100, and Pd-Ru-A-100 were essentially completed, thus concluding chemisorption work for most of the pelletized alloy catalysts. Therefore, it seems appropriate at this point to

TABLE 8

Effects of H_2S on H_2 and CO Chemisorption
for Alumina-Supported Nickel and Nickel Alloys
(10 ppm H_2S at 450°C)

CATALYST	NOMINAL COMPOSITION	H_2 Uptake (μmoles/g) H_2S Exposure			CO Uptake (μmoles/g) H_2S Exposure		
		INITIAL	6 HOURS	12 HOURS	INITIAL	6 HOURS	12 HOURS
Kaiser Al_2O_3	Pure Al_2O_3	0.5	--	--	26.3	31.1	38.9
Inco Ni Powder	Pure Ni	3.47	--	--	5.3[c]	--	--
Ni-A-111	3% Ni	21.4[d]	16.8	14.0	80.0	243.9	373.6
Ni-MoO_3-A-101	2.5% Ni -	24.0[a]	--	--	107.3	260.8	257.6
	3% MoO_3	21.1[b]	13.57	12.45*	--	--	--
MoO_3-A-101	3% MoO_3	1.0	--	--	8.0	8.0	--
Engelhard Ru	0.5% Ru	7.62	5.33	3.45	54.0	45.2	42.5
Ni-Ru-A-105	2.5% Ni -	47.6[a]	--	--	148.2	283.1	295.6
	0.5% Ru	39.4[b]	32.0	25.8	--	--	--
Ni-Rh-A-100	2.5% Ni -	43.5[a]	--	--	145.6	225.8	256.4
	0.5% Rh	38.3[b]	33.5	28.3	--	--	--
Ni-Fe-A-100	10% Ni - 10% Fe	82.13	49.60	42.71	255.1	305.6	393.4
Ni-Co-A-100	10% Ni - 10% Co	114.9	109.6	102.0	176.5	231.3	226.4

*After 24 hours H_2S

[a&b]Refer to different measurements for the same catalyst batch

[b]Data reported in QPR-1

[c]Irreversibly chemisorbed at 25 and -83°C

[d]Reduced in small glass sample cell

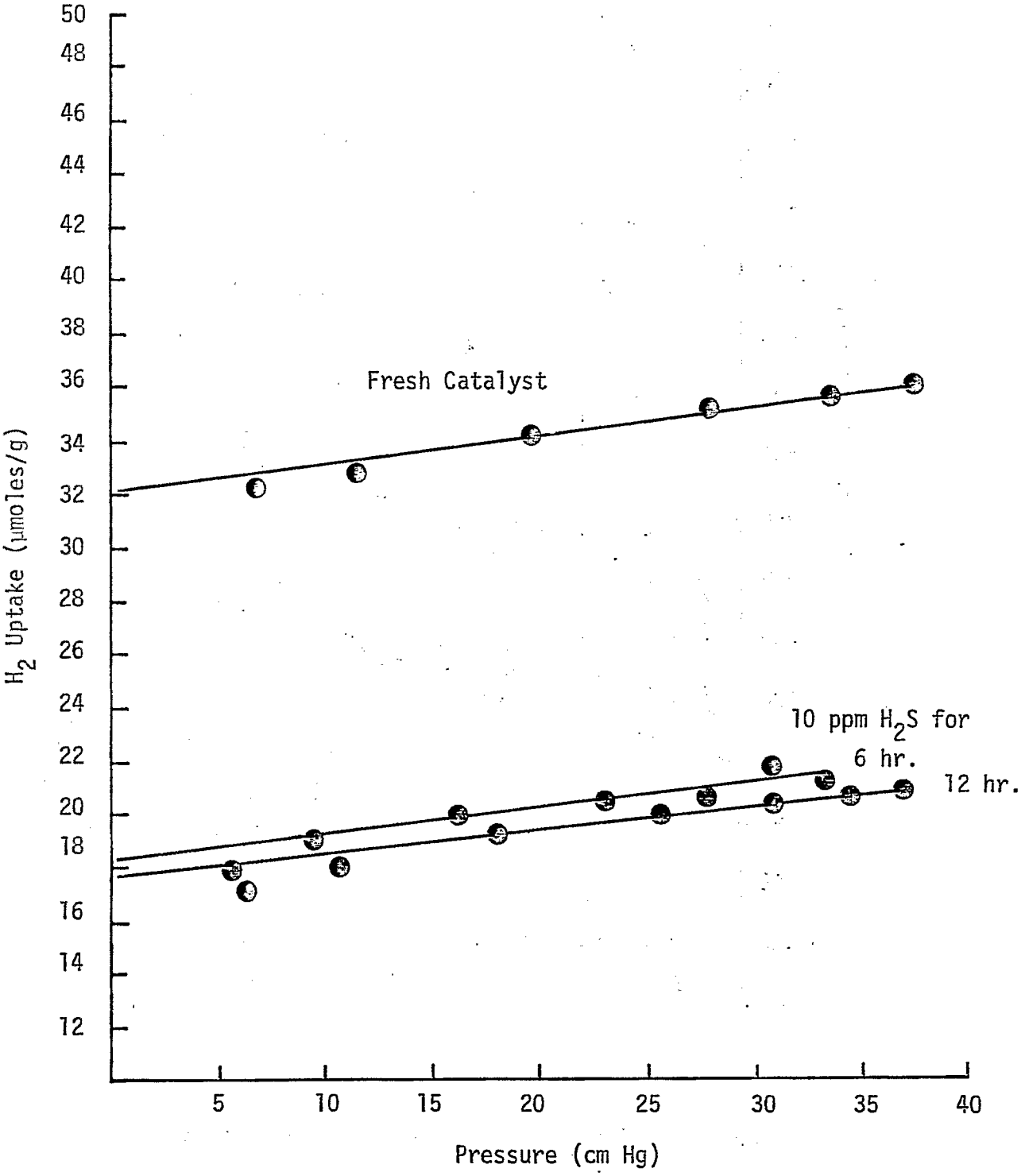

Figure 7. Poisoning of Ni-MoO_3-A-101 with 10 ppm H_2S - Effect on H_2 Chemisorption.

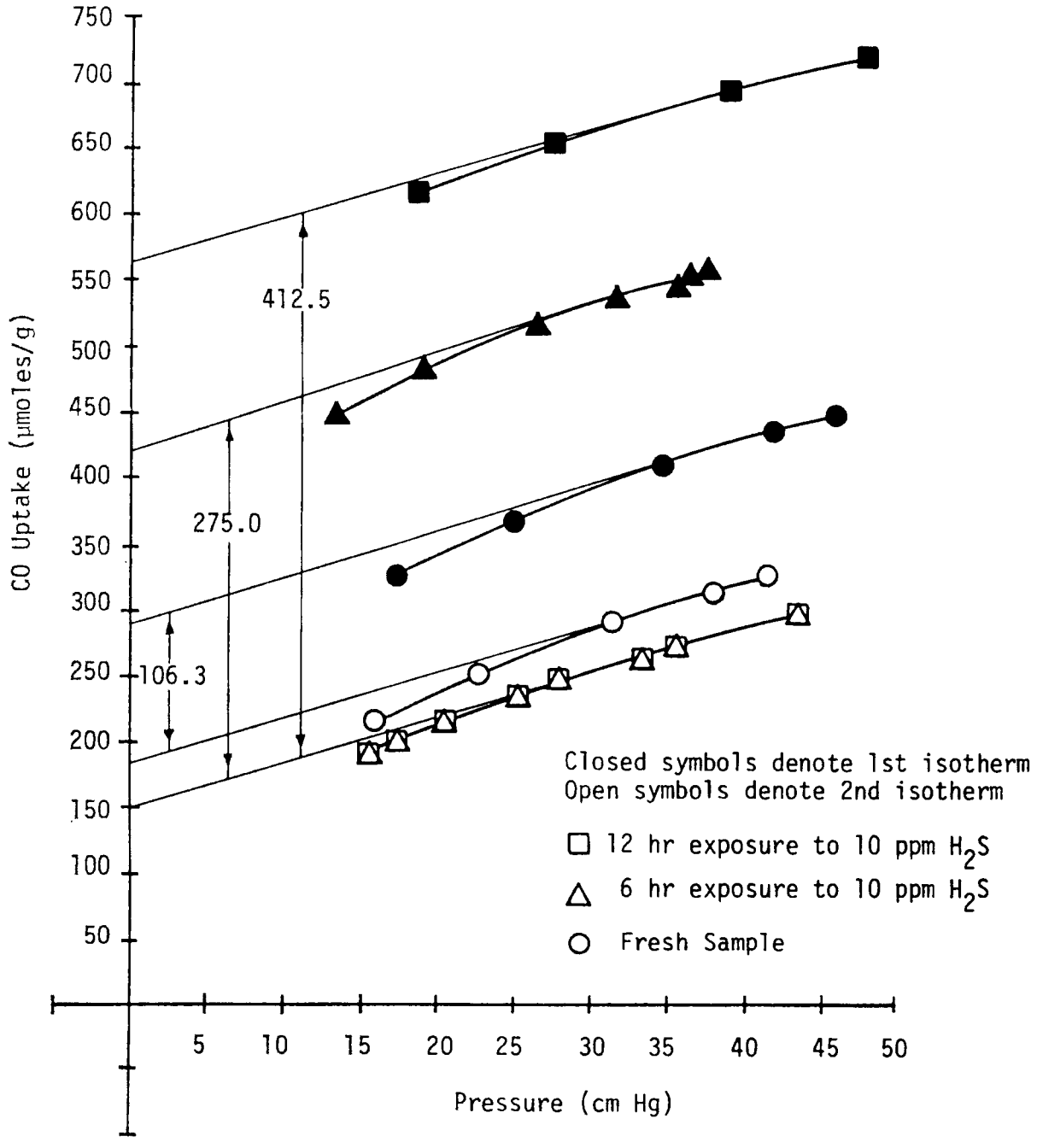

Figure 8. Effects of 10 ppm H_2S on CO Adsorption (-83°C) on Ni-A-111.

make a complete summary of this work.

Previous work (see Table 8) with Ni-Ru, Ni-MoO_3 and Ni-Rh, etc. was not characterized by a constant or specified space velocity; the results from these runs have been reported in QPR-1, QPR-2, and QPR-3 (3-5). As explained in the previous report (5), space velocity is an extremely important variable in poisoning studies, and meaningful comparisons can be made only when this variable is controlled; hence, previous results are only qualitative in nature but do reflect some important trends. The catalysts discussed below were run under conditions such that space velocity, temperature, pressure, and concentration were well-characterized and thus the results can be quantitatively compared.

Before discussing the results in depth, a presentation of a new concept, the poisoning ratio, and its ramifications will be treated. It should be noted the percentage decreases in surface area are not good indicators of relative catalyst performances; however, they do indicate relative trends on a given catalyst. In order to compare different catalysts and their relative resistances to poisoning, it is important to normalize the effects of varying surface areas, dispersions, loadings, poison concentrations, and space velocities. In an attempt to do this, a simple equation was developed to define a quantity called the poisoning ratio:

$$PR = \frac{\text{surface area decrease during poisoning run}}{\text{surface area decrease if all } H_2S \text{ were adsorbed}}$$

The numerator can be calculated from the change in hydrogen chemisorption times the planar density if the surface stoichiometry is assumed. The denominator can be calculated by knowing the amount of poison passed over the catalyst calculated from space velocity, and concentration of the poison and some assumption regarding the site density of the adsorbed sulfur. This ratio also reflects the unit decrease in surface area per unit amount of poison passed over the catalyst. Since temperature, pressure, space velocity, and poison concentration are all held constant, mass transfer coefficients, etc. should be approximately constant and it should be possible to measure relative resistances to poisioning of different catalysts based on the above equation. The applicability of carbon monoxide adsorption as a basis for the poisoning reaction appears to be less desirable than H_2 adsorption in view of the ill-defined stoichiometry and lack of reproducibility of the former.

There are two approaches which may be used to evaluate the poisoning ratio; one based on surface area and one based on hydrogen chemisorption sites:

$$\text{site basis: } PR = \frac{2(n^{\circ}_{H_2} - n_{H_2})\ \rho N_0}{(n_{H_2S})\ (x)\rho\ N_0} = \frac{2(n^{\circ}_{H_2} - n_{H_2})}{n_{H_2S}(x)} \qquad (1)$$

surface area basis: $$PR = \frac{2(n^{\circ}_{H_2} - n_{H_2})\ \rho N_o}{(n_{H_2S})\ s\ N_o} = \frac{2(n^{\circ}_{H_2} - n_{H_2})\rho}{n_{H_2(s)}} \quad (2)$$

where n_{H_2} = hydrogen uptake (moles/g cat.)
n_{H_2S} = H_2S input (moles/g cat.)
ρ = metal planar density ($\AA^2$/atom)
x = fraction of H_2 sites covered by one adsorbed S atom
s = surface area of one adsorbed H_2S molecule ($\AA^2$/atom)
N_o = Avagadros number

It can be seen that the two equations differ only by the factor $x\rho/s$. Using hydrogen chemisorption and sulfur analysis, Rostrup-Nielsen (16) has determined x to be 1.85 for nickel catalysts. Experimental measurements of s have not been made, but some theoretical values have been proposed (17). Of course, the values of s and x will certainly be a function of the metal being studied; clean surface work is not extensive enough for a priori prediction of either. Since no experimental values of s are available, poisoning ratios for this report are based on the first formula; this method should also tend to minimize the effects of uncertainty in planar density calculations.

Tables 9 and 10 summarize the poisoning studies for several nickel and ruthenium alloy catalysts. Representative isotherms are shown for two catalysts in Figures 9 and 10. Hydrogen and carbon monoxide adsorption uptakes were calculated in the previously described manner and formulas for surface area, dispersion, and particle size were discussed in the appendix of QPR-1 (3). Site densities used in the calculations are presented in the appendix of this report. The number in parenthesis listed just after each H_2 uptake value is the percent decrease in surface area for a given 6 or 12 hr. poisoning period, based on initial uptake in all cases. The poisoning ratios were calculated using the site form of the poisoning ratio. All hydrogen adsorption measurements were measured at 25°C except for those catalysts containing palladium and/or ruthenium which were run at 130°C. According to Benson, et al. (18) absorption (reaction with the bulk metal to form a metal hydride) in palladium systems can be avoided by keeping the temperature above 100°C and the pressure below 350 Torr. Figures 11 and 12 show the effects of temperature on adsorption during some recent runs. For the 25°C runs, the adsorption isotherm is concave downward and suggests that uptake increases indefinitely with pressure. Presumably, this is due to absorption as the pressure rises.

All carbon monoxide adsorption isotherms were run at -83°C using the procedure outlined earlier. Correction for support adsorption was made for all runs. The detailed results for each catalyst will be discussed in the order noted in Table 9.

Ni-Fe-A-100. The results for Ni-Fe-A-100 have been discussed in QPR-3 and will not be repeated here; however, the newly calculated poisoning ratios are of interest; and comparison with the other

TABLE 9

Effect of 10 ppm H_2S (GHSV = 2000 hr^{-1}) on H_2 and CO chemisorption

Catalyst	Initial H_2 Uptake	H_2 uptake after 6 hrs poisoning	H_2 uptake after 12 hrs. poisoning	Initial CO Uptake	CO Uptake after 6 hrs poisoning	CO uptake after 12 hrs poisoning	Poisoning Ratios: 6 hrs exposure	Additional 6 hrs. exposure	12 hrs Overal
Ni-Fe-A-100	80.6	49.6 (38)	42.7 (47)	259	302.9	390.7	4.97	1.106	3.04
Ni-Co-A-100	114.9	109.6 (4.6)	102.0 (11)	173.8	228.6	223.7	1.26	1.80	1.53
Ni-Pd-A-100	107.4	107.8 (-0.37)	103.0 (4.1)	145.5	240.0	328.4	-0.0753	0.908	0.416
Ni-Pt-A-100	152	144.0 (5.3)	138.0 (9.2)	139.0	356.0	352.5	1.18	0.891	1.07
Pd-Ru-A-100	21.0	18.0 (14)	6.5 (69)	70.0	57	21.0	0.385	1.48	0.933
Co-Ru-A-100	48.3	35.0 (27)	34.1 (29)	58.5	59	81.0	2.68	0.180	1.43
$Y\text{-}Al_2O_3$	0.5	———	———	48.8	48.8	48.8	———	———	———

H_2 uptakes are not corrected for H_2 chemisorption on support (∿.5 μmoles/g catalyst for these conditions)
Numbers in parentheses indicate the % decrease in uptake for 6 (or 12) hour exposure based on initial uptake.

TABLE 10

Effect of 25ppm H_2S (GHSV = 2000 hr^{-1}) on H_2 and CO chemisorption

Catalyst	Initial H_2 Uptake	H_2 uptake after 6 hrs. poisoning	H_2 uptake after 12 hrs. poisoning	Initial CO Uptake	CO uptake after 6 hrs. poisoning	CO uptake after 12 hrs. poisoning	Poisoning Ratios 6 hrs. exposure	Additional 6 hrs. exposure	12 hrs. overall
Ni-Fe-A-100	118	79.5(33)	73.0(38.1)	274.8	328	372	1.80	0.305	1.06
Ni-Co-A-100+	116	114.4(1.3)	100(13.8)	190.8	243	—	0.151	1.41	0.781
Ni-Pd-A-100++	75	50(33)	66.3(11.6)	142.1	175.5	300.5	2.02	-1.32	0.352
Ni-Pt-A-100+	121.0	107.5(11)	100(21.0)	160.8	363	909	0.778	0.432	0.605
Co-Ru-A-100+	40.4	18.9(53)	29.0(28.2)	104.8	69	56	1.74	-0.816	0.462
γ-Al_2O_3	0.42	0.92	0.5	29	42	60	———	———	———

\+ May be in bulk sulfide forming region - H_2 chemisorption run at 25°C.

++ H_2 adsorption run at 25°C - H_2 chemisorption results are only approximate

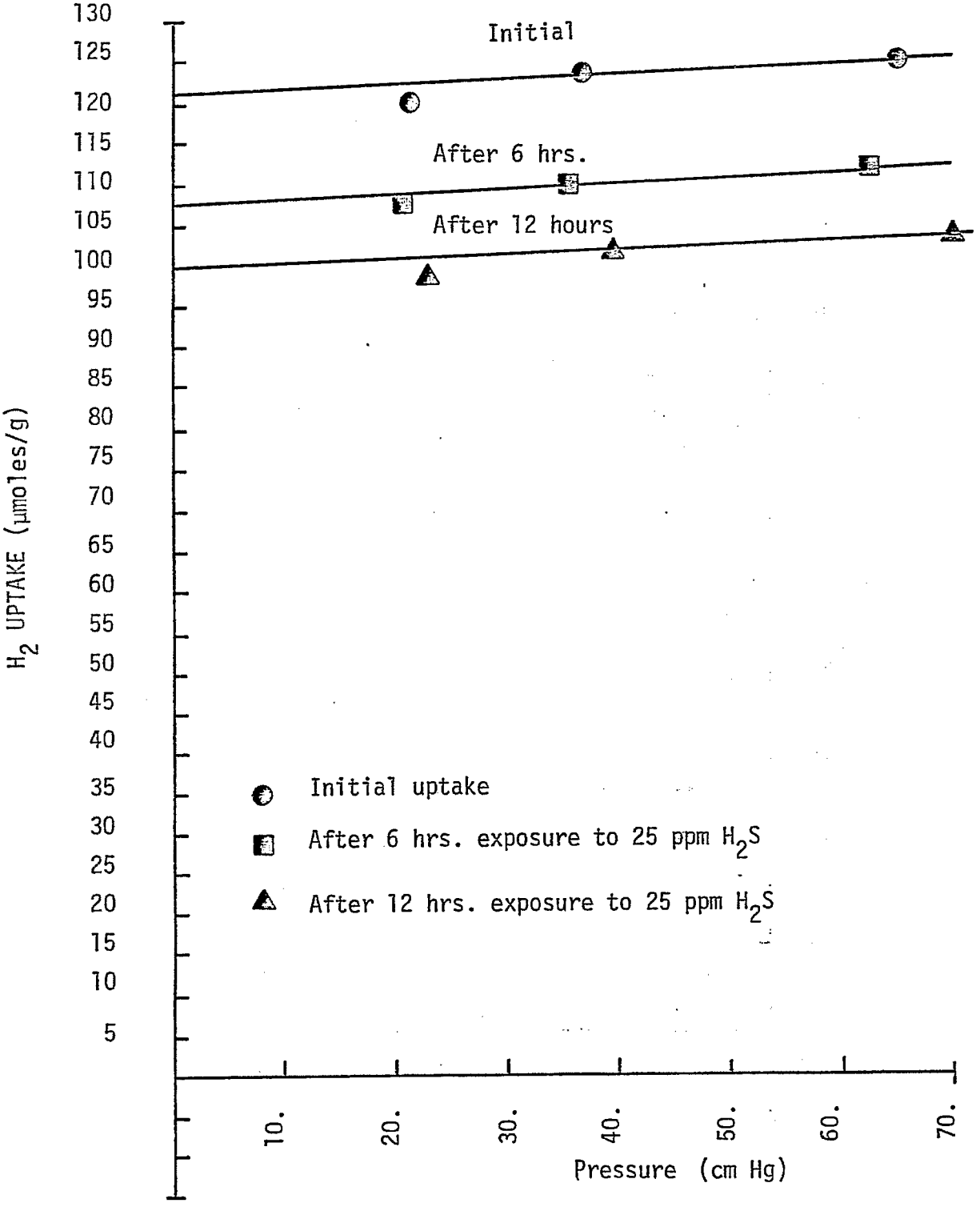

Figure 9. Effects of 25 ppm H_2S on H_2 Adsorption for Ni-Pt-A-100

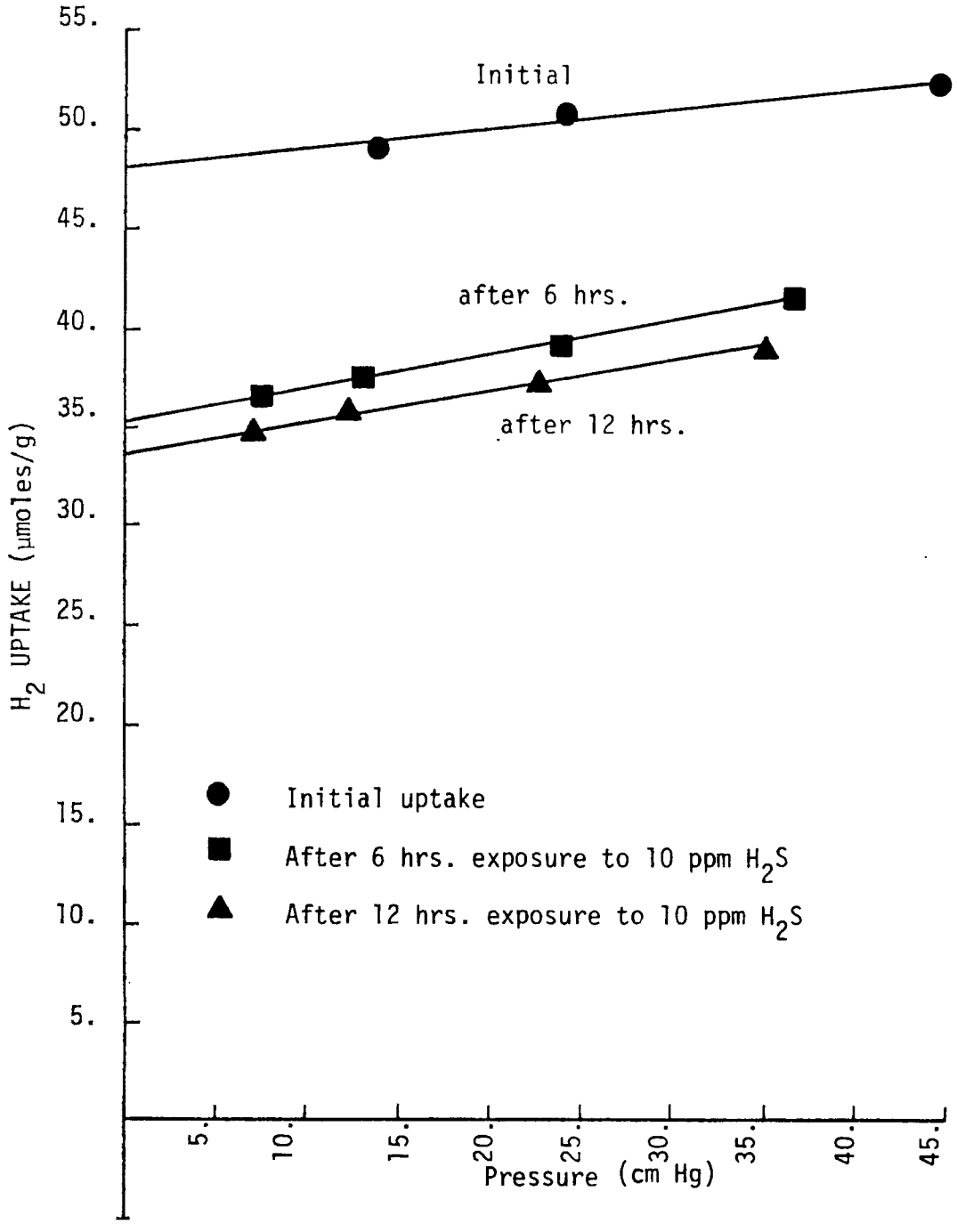

Figure 10. Effects of 10 ppm H_2S on H_2 Adsorption for Ru-Co-A-100

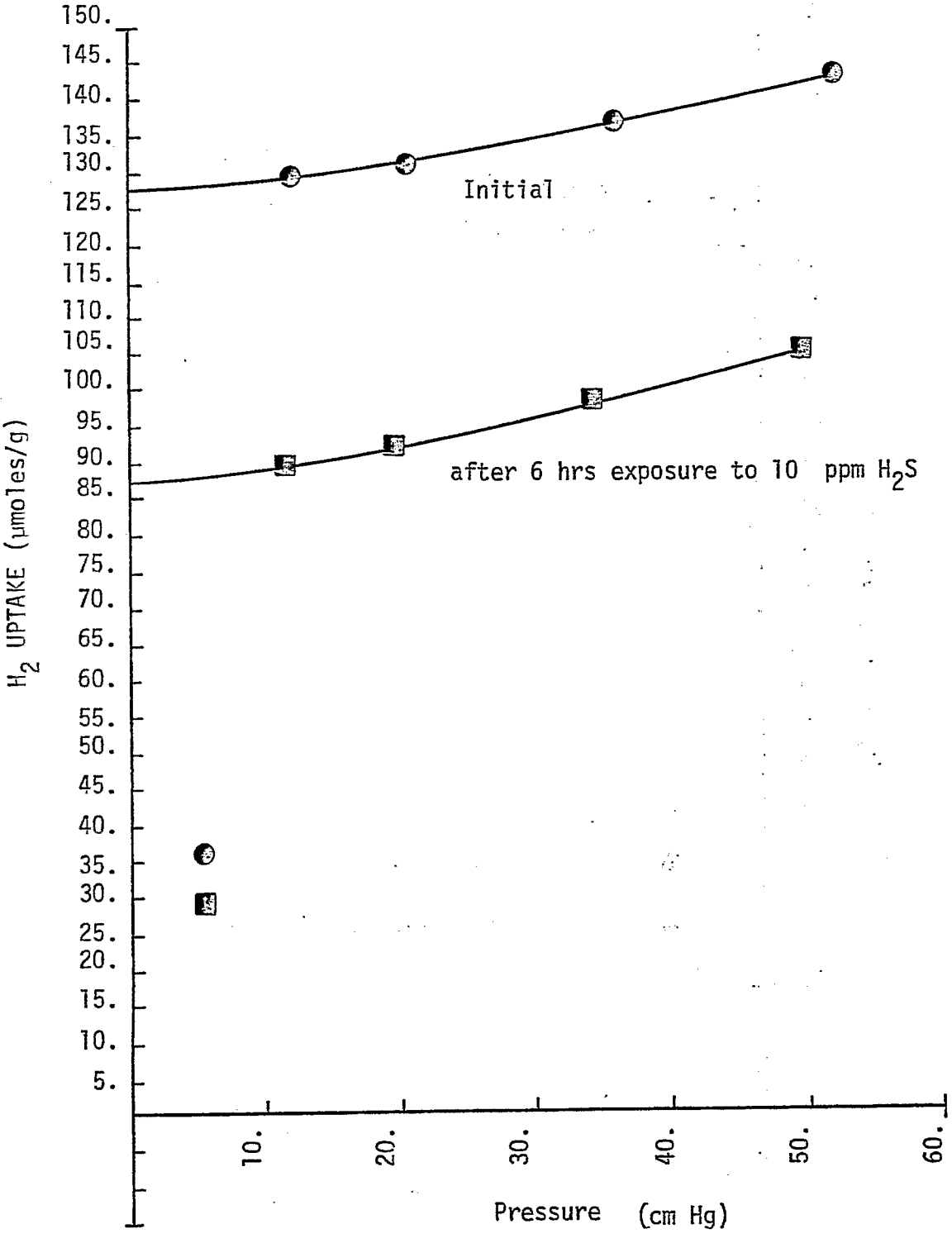

Figure 11. H_2 Adsorption on Ni-Pd-A-100 at 25°C

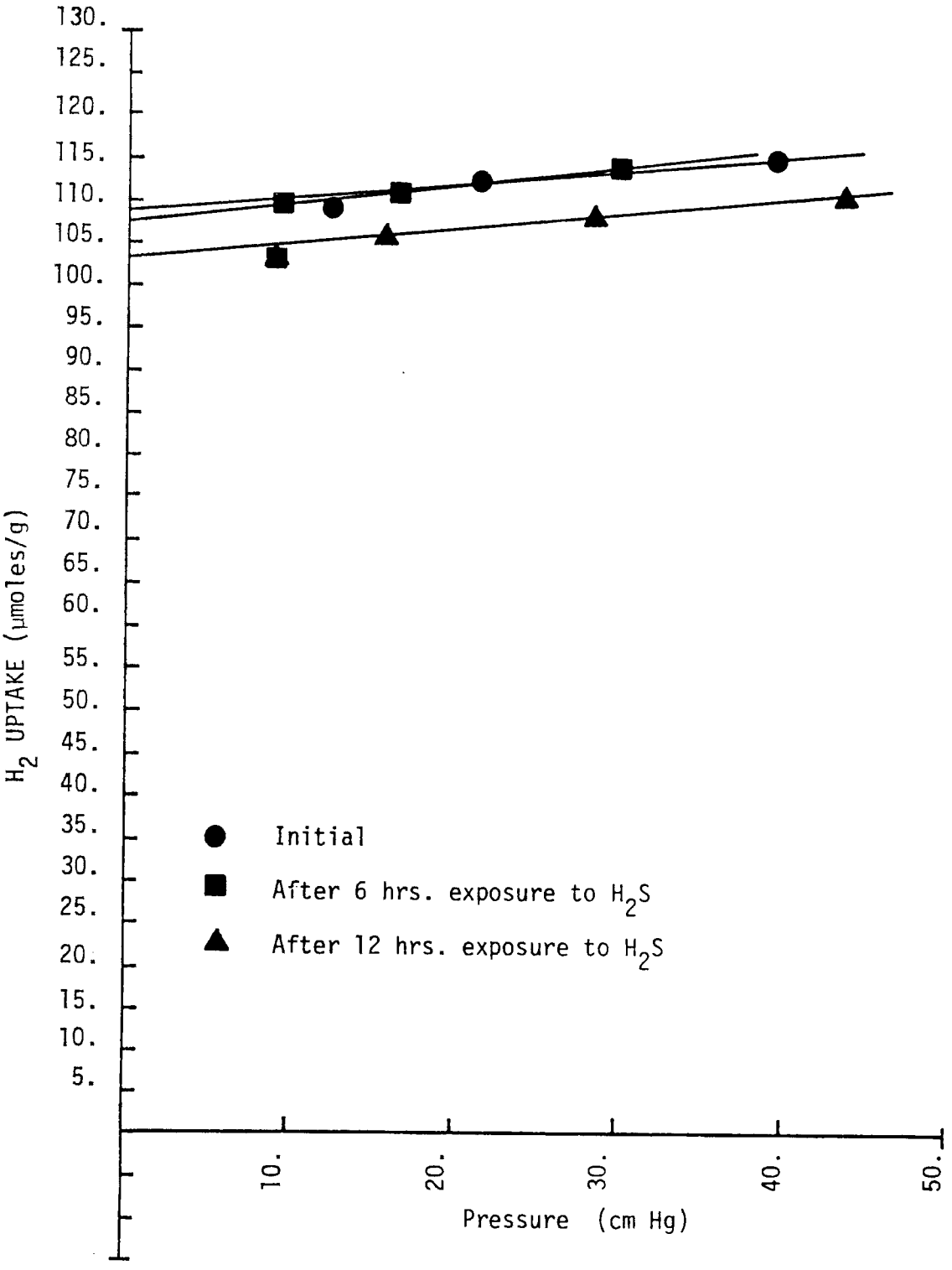

Figure 12. H_2 Adsorption or Ni-Pd-A-100 at 135°C

catalysts indicates Ni-Fe/Al_2O_3 is rather susceptible to sulfur poisoning. The 25 ppm run indicates the nickel-iron catalyst is less sensitive to sulfur poisoning at higher concentration; nevertheless, the overall tolerance is low compared to the other catalysts. Also, it is interesting that the catalyst tends to stabilize after 6 hrs. exposure and is more sulfur resistant thereafter. Indeed, both runs point to this strongly.

Ni-Co-A-100. Some of the results for Ni-Co/Al_2O_3 were discussed in QPR-3; however, results from the 25 ppm runs were only recently available. Poisoning ratios for Ni-Co/Al_2O_3 are too high to look very promising, although this catalyst does show some improvement in the higher H_2S concentration range. It is interesting that the susceptibility to poisoning increases with time for both samples of this catalyst as reflected by the increasing poisoning ratios and percent decreases in uptake based on initial surface area.

Ni-Pd-A-100. Results for Ni-Pd/Al_2O_3 suggest this catalyst has considerable potential sulfur resistance; indeed, for both runs this catalyst has the lowest overall poisoning ratios of any catalyst. However, the poisoning ratio after each 6 hour exposure does not correlate well at the two concentration levels; in fact, the 25 ppm run may be complicated by bulk sulfide effects which could tend to cleave the crystallite and expose new sites to hydrogen adsorption. Since no phase data were available for palladium-sulfur systems, the possibility of these effects cannot be ruled out. The negative poisoning ratio for the 25 ppm run may also be due to experimental inaccuracy, although the 25 ppm poisoning ratios are generally large relative to experimental errors.

Ni-Pt-A-100. The data in Table 9 indicate this catalyst to be moderately resistant to H_2S poisoning. The 25 ppm run for Ni-Pt/Al_2O_3 also suggests this catalyst is quite resistant to sulfur poisoning and the resistance tends to increase with time.

Pd-Ru-A-100. Several experiments with ruthenium and palladium containing catalysts in which erratic results were obtained suggest the inapplicability of 25 ppm sulfur streams in poisoning studies; therefore, data for the 25 ppm runs are not reported for this catalyst. Again, the formation of bulk sulfide of some similar mechanism may explain this difficulty. The data for the 10 ppm run suggest this catalyst may have high initial resistance in sulfur streams; in fact, this catalyst is second only to Ni-Pd/Al_2O_3 in initial sulfur resistance; however, the large decrease in uptake after the second H_2S exposure suggests it may rapidly deactivate after a significant amount of sulfur has adsorbed on the surface.

Co-Ru-A-100. Although the results for the 25 ppm run on this catalyst may be complicated by bulk sulfide formation (especially in light of the negative poisoning ratio), the trends for each run indicate the catalyst may be stabilized after a certain time and further decreases in surface area on exposure may be small.

Al_2O_3. Results for previous alumina runs are discussed extensively in QPR-3 (5); however, the 25 ppm run was not available at that time. Hydrogen adsorption is seen to remain negligible after H_2S exposure. Carbon monoxide adsorption is seen to increase with increasing sulfur exposure; the possible surface interactions for CO and the sulfided support are discussed in QPR-3.

3. X-ray Diffraction and Fluorescence Measurements. The purpose of X-ray diffraction measurements is two-fold: (1) measurement of metal crystallite size and (2) determination of metallic phases for selected catalysts. It is especially important to be able to show if our bimetallic catalysts contain alloys rather than separate metals or oxide phases. X-ray camera measurements for a Ni/Al_2O_3 catalyst were reported in QPR-2 (4). The results showed both Al_2O_3 and nickel metal to be present, but because of diffuse broad lines the photograph was not suitable for estimating particle size. It was hoped that other diffractometers at the University could be used to obtain better resolution.

X-ray diffraction measurements were carried out during the third quarter using a General Electric diffractometer located in Geology and a Phillips diffractometer located in Metallurgy. Both instruments are equipped with goniometers, counting electronics, and chart output. Unfortunately the G.E. instrument is somewhat dated and the detector is simply not sensitive enough for our purposes. In fact, we were unable to separate alumina or nickel peaks from the unstable background. Our experience with the newer Phillips instrument was better. Although the principal (111) peak of nickel was obscured by a broad (400) alumina peak we were able to observe the secondary (200) peak for nickel metal. The background-to-noise ratio was nevertheless poor for the 2°/min scan, but it was apparent from this experiment that we would be able to improve our signal-to-noise ratio by decreasing the scan rate to 0.12°/min. or by counting over long period of time at fixed angles. In other words, the experiment demonstrated that it is feasible to use the Phillips instrument to determine phase composition and particle size for nickel-alumina catalysts. Unfortunately the Phillips instrument will be dedicated solely for metallurgical work during the next few months. Thus, most of our data thus far was obtained using a diffractometer at the University of Utah.

During the last quarter, X-ray diffraction measurements were completed for a number of pelletized nickel and alloy catalysts. Table 11 summarizes results obtained for nickel, nickel alloy, and ruthenium alloy catalysts. The measurements were complicated considerably by the presence in each catalyst of small Al_2O_3 crystallites (about 50 A in diameter) causing numerous intense peaks. In many cases, the line broadening due to the Al_2O_3 support made identification difficult or impossible for a number of metal peaks. In the following discussion, diffraction peaks will be identified by their d values as calculated from the Bragg equation; constants for the alloys were taken from an extensive summary by Pearson (19). The probable error in d values was estimated from the total derivatives of d

with respect to θ in the Bragg equation, and it was found that the expected error in d increased from .002 Å to .03 Å as θ was varied from 60° to 20°.

X-ray diffraction data are presented for three different nickel catalysts of 9, 13.5, and 25 wt.% in Table 11. The data establish the concentrations for which nickel particles are observable in the alumina matrix. No nickel lines were observed for the 9% nickel catalyst and the two observable nickel lines for the 13.5% sample were very weak. Two nickel peaks were moderately observable for the 25 wt.% nickel on Al_2O_3. In all cases the intense, broad Al_2O_3 peak at 1.98 Å obscures the most intense nickel peak (usually observed at 2.03 Å). Nevertheless, it was possible to calculate nickel crystallite diameters for the 13.5 and 25% samples using the Sherrer Equation (20) and the line broadening for the (200) and (220) peaks at 1.77 and 1.25 Å respectively.

The crystallite diameters calculated from x-ray line broadening are shown in Table 12 and compared with crystallite diameters calculated from hydrogen chemisorption. Apparently fair agreement is obtained between the values determined for the 25% sample from x-ray diffraction (200 peak) and from chemisorption. The significantly lower value from x-ray for the (220) peak of the 25% sample suggests that the particle shape is not regular. The particle size from x-ray for the 13.5% sample is also lower than determined from chemisorption. Normally it is expected that particle diameter calculated from x-ray line broadening will be larger than for those calculated from chemisorption since the former is a volume averaged property and the latter a surface area averaged property. This discrepancy might be explained by consideration of the effects of non-reduced nickel which is known to occur in Ni/Al_2O_3 catalysts (7). It has been observed that the percent reduction to nickel metal increases and that percent dispersion decreases with increased metal loading. If we suppose that this unreduced nickel occupies a portion of the surface of each crystallite or is even situated separately from the reduced metal crystallites, then the particle diameter calculated from hydrogen chemisorption will be <u>higher</u> than the true diameter since hydrogen does not adsorb on the nickel oxide sites and since our calculation assumes that hydrogen adsorbs on every available metal surface site. This model predicts an increasing discrepancy between x-ray and chemisorption calculations as the metal loading and percent reduction to nickel metal are decreased. Indeed the data are consistent with this view. It is also expected that better agreement will be found for Ni-Pd and Ni-Pt catalysts where nickel is believed to be essentially metallic. In fact, data in Table 12 for Ni-Pt do show slightly better agreement between the two methods. Exceptionally good agreement is obtained in the case of Ni-Co-A-100.

There were only three significant peaks for the Ni-Fe-A-100 catalyst as most of the metallic peaks were partially or wholly obscured by alumina interference. A very weak peak at 1.773 Å suggests the existence of either nickel (200) or the alloy (200) plane or both. Weak peaks at 2.034 Å and 2.079 Å correspond to the d values

TABLE 11

X-ray Diffraction Peak Assignments

Catalyst	d- value (Å)	Assignment
Ni-A-113 (9% Ni)	1.40	γ-Al_2O_3 very strong
	1.52	γ-Al_2O_3 very weak
	1.99	γ-Al_2O_3 strong
Ni-A-114 (13.5% Ni)	1.251	Nickel (220) very broad and weak
	1.40	γ-Al_2O very strong
	1.76	Nickel (200) very broad & weak
	1.99	γ-Al_2O_3 very strong
Ni-A-115 (25%)	1.25	Nickel (220) moderate-strong
	1.405	γ-Al_2O_3 strong
	1.433	? moderate
	1.495	γ-Al_2O_3 (?) moderate diffuse
	1.769	Nickel (200) moderate-strong
	2.056	γ-Al_2O_3 very strong
Ni-Fe-A-100	1.142	γ-Al_2O_3 weak
	1.399	γ-Al_2O_3 strong
	1.773	alloy (200) or Nickel (200) very very weak
	1.963 thru 1.987	γ-Al_2O_3 strong
	2.034	Nickel (111) weak
	2.079	alloy weak
	2.296	γ-Al_2O_3 weak
	2.430	γ-Al_2O_3 moderately strong
Ni-Co-A-100	1.25	Nickel (220) and/or Cobalt (110) very weak
	1.40	γ-Al_2O_3 strong
	1.48	Cobalt (102) very weak
	1.77	Nickel (200) very weak
	1.98	γ-Al_2O_3 strong

(Table 11 - Contd.)

Catalyst	d- value	Assignment
Ni-Co-A-100	2.03 - 2.09	Alloy (111) Nickel (111) and/or Cobalt (002) moderate.
	2.44	Alloy (101) or alloy (110) or γ-Al_2O_3
Ni-Pt-A-100	1.14	γ-Al_2O_3 very weak
	1.25	Nickel (220) or alloy (220) weak-moderate
	1.40	γ-Al_2O_3 strong
	1.77	Nickel (200) and/or alloy (200) moderate
	1.979	γ-Al_2O_3 strong
	2.034	alloy (111) or/and Nickel (200) very strong
	2.279	γ-Al_2O_3 weak
	2.402	γ-Al_2O_3 moderate
	2.761	γ-Al_2O_3 weak
	2.976	? weak - moderate
Ni-Pd-A-100	1.250	Nickel (220) moderate-weak
	1.401	γ-Al_2O_3 strong
	1.78	alloy (200) or Nickel (200) moderate strong
	1.979	γ-Al_2O_3 strong
	2.034	alloy (111) or Nickel (111) very, very strong
	2.29	γ-Al_2O_3 weak
	2.41	γ-Al_2O_3 moderate
Ru-Co-A-100	1.25	Cobalt (110) weak
	1.395	γ-Al_2O_3 moderate - strong
	1.4296	γ-Al_2O_3 weak
	1.96	γ-Al_2O_3 Cobalt (101) moderate
	2.03	Cobalt (002) and/or moderate Ruthenium (101)
	2.17	Ruthenium (002) Cobalt (100) weak

Table 12. Comparison of Particle Sizes Calculated from X-ray Line Broadening and Hydrogen Adsorption

Catalyst	X-ray plane	d particle (Å) from X-ray	d particle (Å) From H_2 Adsorption
Ni-A-115 (25%Ni/Al_2O_3)	(200)	53.2	65.3
	(220)	36.4	
Ni-A-114 (13.5% Ni/Al_2O_3)	(200)	32.3	46.4
Ni-Fe-A-100	no easily distinguishable peaks		
Ni-Co-A-100	(200)	95.3	99.1
	(102)	77.7	
	(225) or (110)	88.8	
Ni-Pt-A-100	(111)	75.3	86.6
	(200)	67.9	
	(220)	78.8	
Ni-Pd-A-100	(200)	75.4	115
	(220)	89.2	
Ru-Co-A-100	(002) or (100)	121.6	253
	(110)	108.6	

of the nickel (111) and the alloy (111) plane, respectively. It is interesting that the peak at about 2.0 Å for Ni-A-115 is symmetric and shows no evidence of subpeaks at 2.079 Å. Therefore, the Ni and Ni-Fe peaks at 2.034 and 2.079 Å suggests the possible presence of both alloy (111) and nickel (111) planes in the crystallites. Nevertheless, none of the metal peaks was sufficiently distinguishable to enable particle size to be determined.

The diffractogram for Ni-Co-A-100 suggests the presence of nickel (220) and cobalt (110) planes at 1.25 Å, although the amounts appear very small in view of the small peak size. Very weak peaks for the individual metals corresponding to the cobalt (102) and nickel (200) planes occur at 1.48 Å and 1.77 Å respectively. Several peaks at 2.03 Å and 2.09 Å, similar to those observed for Ni-Fe-A-100, suggest also the presence of the alloy (111), cobalt (102), and nickel (111) planes. A large peak at 2.44 Å corresponds to the alloy (111) and (101) planes; however, this peak may also be due to the Al_2O_3 peak at 2.39 Å. Comparison of this peak with a nickel sample was not possible because the nickel runs started with d = 2.2 Å.

A small peak at 1.25 Å on the Ni-Pt-A-100 diffractogram suggests the presence of the alloy (220) and/or nickel (220) planes. A larger peak at 1.77 Å suggests the presence of alloy (200) and/or nickel (200) planes. The presence of such small amounts of platinum makes it difficult to decide which plane is the predominant contributor to the peak. A very large peak at 2.034 Å may be due to the nickel (200) and/or the alloy (111) planes. It is important that the corresponding peak for the Ni-A-114 catalyst is entirely absent; because of the higher intensity usually associated with high electron density metals, e.g. platinum and palladium, this observation of enhanced peak intensity strongly suggests the formation of a nickel-platinum solid solution or alloy.

The diffractogram for Ni-Pd-A-100 was very similar to that of Ni-Pt-A-100. A moderate peak at 1.25 Å, however, suggests the possibility of nickel (220) planes. A larger peak at 1.78 Å is indicative of the alloy (200) and/or the nickel (200) planes. A very strong peak at 2.034 Å suggests the presence of alloy (111) and nickel (111) planes. Again, the peaks at 1.78 Å and 2.034 Å for Ni-Pd-A-100 were much stronger than the peaks observed for Ni-A-114 and Ni-A-115, suggesting a solid solution is formed between nickel and the noble metal, which significantly increases the peak intensity of the nickel.

The results for Co-Ru-A-100 catalyst indicate cobalt (110) and (101) planes are present for d = 1.25 and 1.96 Å, however, the latter peak is strongly influenced by a nearby Al_2O_3 peak, and the intensity of the cobalt (101) plane is not known. A peak at 2.03 Å suggests that cobalt (102) and/or ruthenium (101) planes are present, and another peak at 2.17 Å suggests ruthenium (002) and/or cobalt (100) planes are also present; however, there are no calculated alloy peaks at these locations.

In summary, evidence for alloy formation is not conclusive for any of the alloy samples although a number of observations support this conclusion; on the other hand, there is very little evidence suggesting that alloys were not formed in any of the alloy catalysts examined. In the case of Ni-Co and Ru-Co several weak Co peaks were identified, however, generally these peaks were very small in intensity. Separation and identification of alloy peaks is complicated by several factors: (1) some alloy peaks occur very close to peaks for one of the constituent metals, and differentiation of the metal from the alloy in this case is not possible, (2) some of the alloys are characterized by only a small amount of one of the metal constituents; hence, the alloy behaves similar to the metal in predominant concentration, and (3) interfering broad alumina peaks obscure many of the important metal peaks. From the data it is inferred that crystallite alloys are probably the predominant metallic structure in the alloy catalysts; however, the presence of small amounts of pure metals cannot be ruled out.

X-ray fluorescence measurements have been initiated for Ni/Al_2O_3 catalysts to determine quantitatively and routinely the chemical composition of our samples. Thus far we have learned how to use the University spectrometer and have prepared and run a standard calibration curve (5) for Ni and Al.

As part of our chemical analysis work two alumina-supported nickel catalysts, Ni-A-113 and Ni-A-114, having nominal compositions of 9 and 15 wt.% respectively, were submitted to Gulf Research for chemical analysis. The analysis revealed 7.55 and 13.53 wt.% nickel. Thus, these nickel catalysts actually contain 10-15% less nickel than expected by assuming that all of the nickel nitrate originally present in the impregnation solution had been transferred to the alumina pellets. This assumption is clearly approximate since in each preparation a small portion of the nickel nitrate is left on the bottom and walls of the breaker after impregnation and drying; indeed, this small portion might account for the 10-15% nickel lost in the preparation. Other samples have been submitted to Corning Glass Works and Engelhard for chemical analysis.

4. Work Forecast. During the next quarter we will tie up the loose ends on the characterization of pellet-supported catalysts and initiate preparation of and characterization of monolithic-supported alloys. X-ray fluorescence measurements will be carried out for Ni/Al_2O_3 and selected nickel alloy catalysts to determine chemical composition.

B. Task 2: Laboratory Reactor Construction

1. Reactor Design and Construction. At the beginning of the contract period we had operational in our laboratory a continuous flow reactor system for catalyst screening and measurement of methanation catalyst activity at either high (integral) or low (differential) conversions over a pressure range of 0-60 psig. As part of this

study the system has been redesigned to (1) allow for operation to 400 psig, (2) significantly upgrade the system with the addition of mass flow meters, a new furnace with temperature programming, and a continuous temperature recorder, and (3) improve the analysis of gaseous products with the addition of a continuous CO-detector, a gas concentration calibration system, and chromatographic accessories to allow accurate measurement of all reactants and products. A schematic of the completed reactor system is presented in Figure 13.

The reactor system is designed such that various concentrations of desired reactant gases can be mixed with or without steam in the pressure range of 0-400 psig and at any temperature from 25-1000°C. The catalyst sample may be of either pellet or monolithic form, of any sample size from 2 ml to 100 ml. Small sample sizes are used in differential testing and large sizes are used for integral testing.

Reaction conditions are monitored in the following ways. Pressure is controlled by high pressure cylinder regulators and a back pressure regulator. Temperature is sensed by a type K (chromel-alumel) thermocouple inserted in the reactor bed. The signal is continuously recorded by means of a Hewlett-Packard #7132 2-pen laboratory strip chart recorder. Flow rates are read with a Matheson mass flowmeter system incorporating five stainless steel transducers with digital readout. The reactor furnace temperature is programmed and controlled using electronics designed and constructed by the BYU Chemistry Instrument Shop. This instrument coupled with a Lindberg 24-inch zone furnace allows 2% control of catalyst sample temperature from 25°C to 1000°C, incorporating programmable temperature-time ramps and constant temperature holds.

The reactant and/or product streams are continuously analyzed for CO using a Beckman model 864-12 NDIR analyzer and then routed to a Hewlett-Packard gas chromatograph model #5830 for periodic sampling and analysis for H_2, CO, CH_4, CO_2, H_2S, and hydrocarbons. The chromatograph with the addition of new accessories features digital control for automatic operation, sub-ambient temperature programming, column switching, and internal or external standard methods of calibration.

To facilitate investigation of the effects of steam on catalyst activity and surface area a water vaporizer has been designed and fabricated. The vaporizer consists of an eight-inch length of three-quarter inch schedule 40 stainless steel pipe into which has been inserted a six-inch length of perforated 1/4" stainless steel tubing which is stuffed with a glass wool wick. Reactant gases enter at the wick end of the pipe and leave after picking up water vapor. The vaporizer and all downstream components to the reactor are wrapped with heating tape and insulation. The vaporizer is maintained at a temperature of 400°C and the downstream components and tubing at 100°C. The water is metered by a Milton-Roy mini pump into the perforated tube where it is carried the length of the tube by capillary action, vaporized, and mixed with other reactant gases before entering

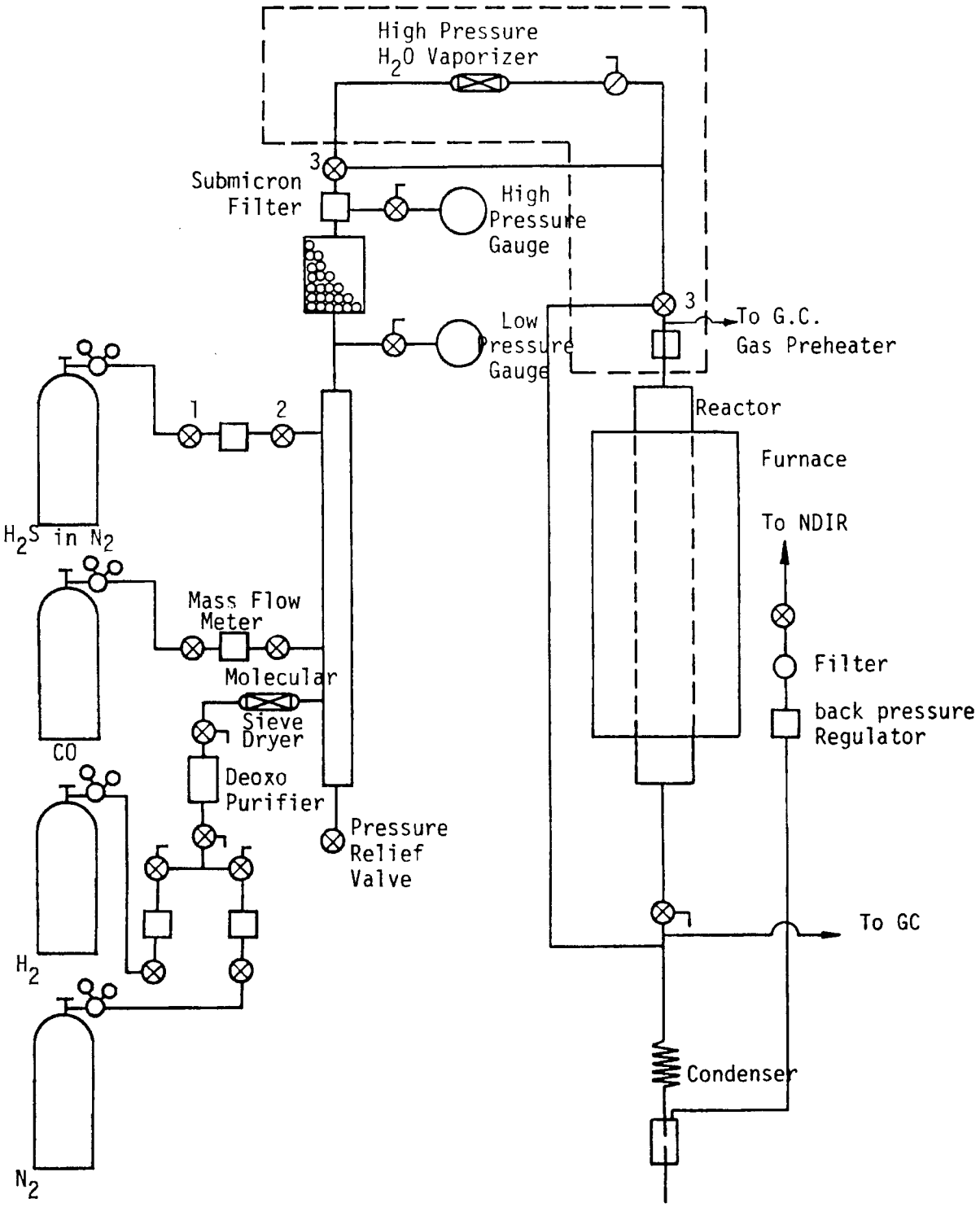

1 S.S. Micro Valve
2 Toggle Valves
3 3-way Valves

The area enclosed in dotted lines will be wrapped with heating tape and asbestos cloth.

Figure 13. High Pressure Laboratory Reactor

the reactor.

The reactor is a stainless steel tube (see Figure 14) with an inside diameter of one-inch and a length of 26 inches. Centered at the outlet end of the reactor is a thermocouple well through which a thermocouple may be extended up into the sample zone of the reactor. This thermocouple may be placed at any desired position along the central axis of the bed. The reactor inlet is flanged so the reactor may be opened for charging or removal of samples. To insure a uniform gas temperature entering the catalyst bed, the gases entering the reactor are preheated by passing through tubing coiled around a portion of the reactor which contacts the furnace. Two such reactors have been fabricated with a shut off valve at each end so that catalyst pretreatment and reduction can be carried out for a sample using our separate reduction system while running simultaneously on the reactor system an already pretreated and reduced sample. Thus use of our reactor system is at least twice as efficient.

During the past quarter various modifications were completed on the reactor system and it is at present operational. The change in the gas sampling technique discussed in QPR-3 (5) has been made such that operation of the reactor need not be interrupted to sample either reactant or product gas streams. In the 4 or 5 runs done since this modification, this new technique seems to work quite well. Figure 15 shows a schematic diagram of the gas sampling section.

The temperature controller-programmer constructed by the BYU chemistry instrument shop is working very satisfactorily. Calibration of the mass flow meter system was completed with some discouraging results. It seems that most of the calibrations done by Matheson were in error due to faulty circuit boards installed at the factory. We have returned 3 mass flow transducers for repair and one has been returned to us. Presently we are operating with 2 mass flow transducers using our own calibration and one which was returned to us recalibrated by Matheson Gas Products.

Other modifications included installation of a back pressure regulator after the reactor to control the pressure in the reactor itself, and replacement of all low pressure lines and valves to allow operation at 400 psig. Also, a column switching device has been installed in the gas chromatograph to facilitate analysis for CO_2. A preheater of coiled 1/4 inch steel tubing was fabricated so that any temperature variations across the catalyst bed would be minimized. As the repaired mass flow transducers arrive, they will be placed in operation. The only work remaining to be done is insertion of the already fabricated steam generator into the reactant line as it is needed.

2. Design and Construction of a Dilution Calibration Apparatus.

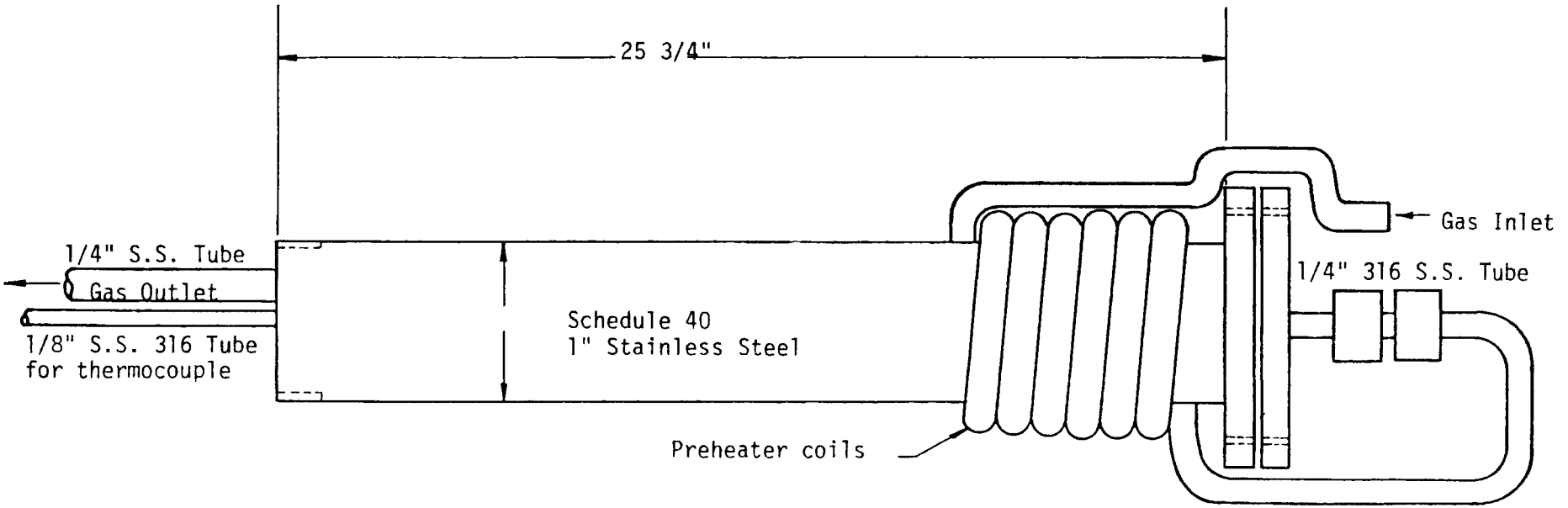

Figure 14. High Pressure Stainless Steel Reactor for Catalyst Testing.

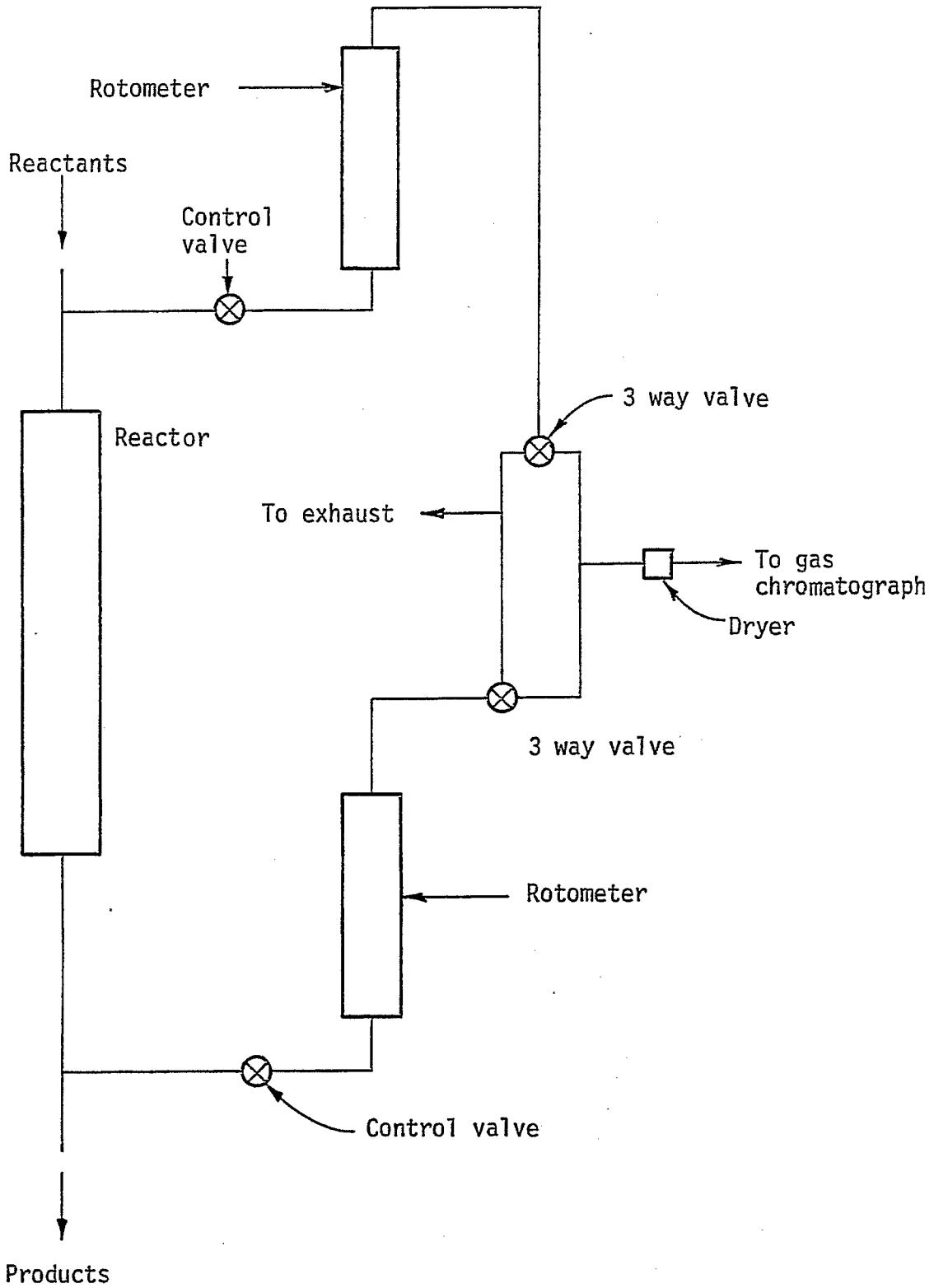

Figure 15. Sampling system for Laboratory Reactor

The design and construction of a dilution apparatus was necessary for the calibration of the gas chromatograph (G.C.). The dilution technique allows calibration gas mixtures to be prepared in various concentrations by dilution with a high degree of accuracy. By injecting known dilutions into the G.C. for analysis, the chromatographic areas of reactant and product mixtures can be related to concentration on a daily basis. Using this technique, very low concentrations can be accurately achieved. The plexiglass dilution chamber with magnetic stirrer was described in considerable detail in QPR-1 (3). This apparatus has already been used in the preparation of calibration standards for our chromatograph.

C. Task 3: Reactor Screening of Alloy Catalysts

1. Design of Screening and Activity Tests

a. Introduction. During the first quarter considerable effort was directed toward designing and refining tests for catalyst screening and measurement of methanation activity. A screening test was designed to give a quick, but useful comparison of catalyst methanation activity under steady-state, reaction-limited conditions using a continuous flow system at atmospheric pressure. The pulse technique was abandoned because (1) earlier experiments in this laboratory showed that pulse broadening in our reactor (especially with monolithic samples) was a serious problem and (2) pulse reactor data cannot be used for calculating steady-state reaction rates for comparison with data by other workers. A procedure for measuring conversion versus temperature was also tested with the purpose of obtaining useful design data for selected catalysts in an integral plug flow system. Both the screening (differential) and integral tests are discussed below followed by a brief discussion of data collection and reduction procedures.

b. Differential test (low conversion screening test). Most catalysts are initially reduced and passivated in our catalyst reduction system. A previously reduced sample of catalyst (usually one to four grams) is loaded into the stainless steel reactor. The sample is heated in flowing H_2 (approximately 500 cm^3/min) to 450°C and held for two hours at that temperature. The sample is then allowed to cool in flowing H_2 to about 225°C. Reactant gases (1% CO, 4% H_2 and 95% N_2) are next allowed to flow through the reactor at a space velocity of 30,000 or 60,000 hr^{-1} for 30 minutes during which time the reactor temperature is stabilized at 225, 250, or 275°C. Reactor pressure is usually about 5-8 psig for screening tests. Three chromatographic samples of the product gas are taken after which three additional chromatographic samples are taken to determine unconverted reactant gas concentrations. All important experimental conditions such as temperature and pressure are recorded at the time each chromatographic sample is taken.

The data are next reduced and the following quantities are calculated: a) conversion of CO to products, b) production of CH_4,

c) production of other species such as CO_2 and other hydrocarbons, d) selectivity, the ratio of b to a, e) rate of CH_4 production and CO conversion per unit weight, f) turnover number, the number of product molecules produced per atomic catalytic site per second based on both CO conversion and CH_4 production.

c. Integral test (high conversion test). The reactor is loaded with a 20-35 cm^3 sample of previously reduced and passivated catalyst. The sample is heated under flowing H_2 to 450°C, held constant at this temperature for two hours and then cooled to 200°C. A reactant gas mixture (1% CO, 4% H_2 and 95% N_2) next enters the reactor at a space velocity of 15,000 hr^{-1} and the reactor is heated at a slow rate (3-5°C per minute). Gas chromatographic samples are taken every 25°C over the temperature range 200°C-475°C. After the run is complete the three chromatographic samples of the unconverted reactant gas are analyzed. The resulting data are plotted as conversion vs. temperature.

d. Testing of poisoned catalysts. The catalysts are reduced in H_2 and exposed to a stream containing various H_2S concentrations from 1-50 ppm in a special pyrex system (see Figure 3) for a period of 6-24 hours. A sample of the poisoned catalyst is charged to the stainless steel reactor and tests are carried out under either differential or integral conditions as previously outlined. Catalysts can also be exposed to H_2S in situ using a special quartz reactor constructed for poisoning and sintering studies.

e. Data collection and reduction. Reactor test data for each run are recorded on reactor test data sheets (3). Similar data sheets are used for recording adsorption data and summary data (composition, physical properties, and test results) for each catalyst.

In order to calculate reactor flow rates and basic kinetic data (conversion, rate, and turnover number) with greater speed and accuracy, interacting calculator programs have been written for use on a Hewlett-Packard 9810 calculator equipped with a Plotter/Alpha ROM and a printer option. These programs recorded on magnetic cards are designed to request specific data input from the user and to provide a hard copy output of all input and ouput, significantly reducing the possibility of error in calculation. Similar programs have also been written for calculation of gas uptakes from adsorption data.

2. Results.

a. Differential screening tests. Initial activity studies were conducted on selected catalysts using the atmospheric pressure reactor shown in Figure 16 surrounded by a 6-inch zone furnace controlled with a simple variac. Since there was no preheater and the heating zone was relatively small, there was a significant temperature gradient across the reactor. The temperature gradient across the differential bed was small, however, and on the order of a few degrees.

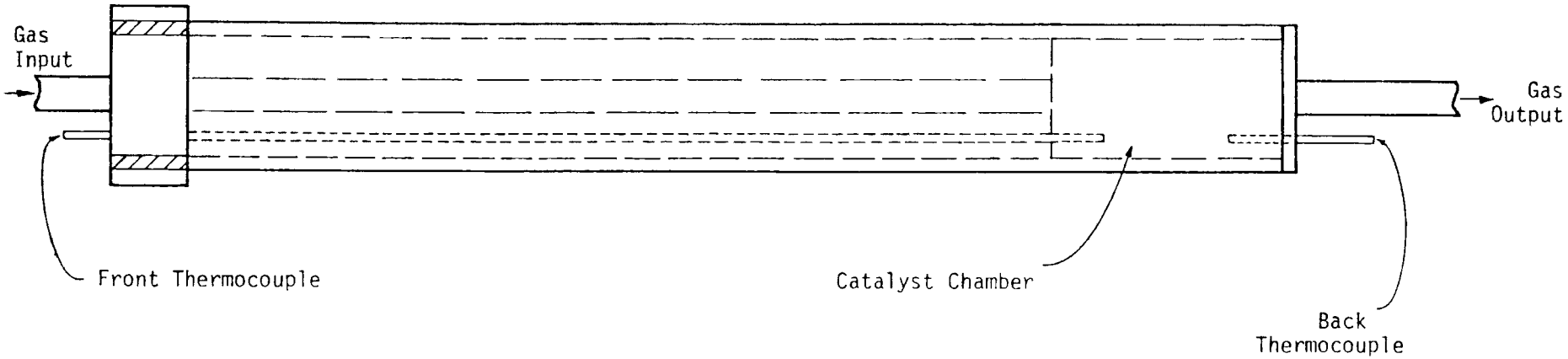

Figure 16. Stainless Steel Catalyst Reactor

(0-60 psig operation)

Specific rates at 275°C and atmospheric pressure for nickel, nickel-ruthenium and nickel-rhodium catalysts supported on 1/8 inch alumina beads obtained during the first quarter are shown in Table 13. Data at 225 and 250°C (1 atm) for nickel and nickel alloy catalysts obtained during the second quarter using the same reactor and furnace are shown in Tables 14-17. Also included in Tables 14 and 16 are recent data for Ni-Cu-A-100, Ru-Pt-A-100 and Ni-Co-A-100 obtained during the fourth quarter using the newly improved reactor system with new reactor and 24-inch zone furnace with preheater. The entering reaction mixture contained 1% CO, 4% H_2, and the remainder was N_2. The rates were determined at low conversions, low temperatures, and high space velocity (225, 250, and 275°C, 3-30% conversion, GHSV = 30,000 and 60,000 hr^{-1}) with 2 to 4 grams of catalyst in the reactor (the remainder of the bed was filled with pure Al_2O_3 pellets) in order to minimize the influence of heat and mass transfer. Catalyst samples were initially reduced at 450-500°C for 6-12 hours before activity measurements were carried out.

The turnover numbers (N_{CO} and N_{CH4}) shown in Table 13 indicate approximately the same order of magnitude activity for Ni, Ni-Ru, and Ni-Rh catalysts. Our turnover numbers agree well with the initial rates reported by Dalla Betta et al. (21) and Vannice (22) for 0.5% Ru/Al_2O_3 and 5% Ni/Al_2O_3. After analyzing the data, it appears that a small uncertainty (1-5%) in our results may be attributed to small variations in gas concentrations, pressure and flow rates over the test period of a given catalyst. The measurement of both activity and selectivity also includes uncertainties of 1-5% in calibration and measurement of gas concentrations. Thus, it may be possible that selectivities for CH_4 are slightly higher than indicated, although there is undoubtedly significant hydrocarbon and CO_2 production (21,22). Efforts were made during the 2nd, 3rd, and 4th quarters to refine our methods of measurement, calibration, and analysis of the data including analysis for CO_2 and hydrocarbons.

Dalla Betta et al. (23) have indicated that their steady-state rates for methanation (after a 24-hour exposure to a reaction mixture) are 25 times lower than their initial rates (21) shown in Table 13. Thus, exposure to a reaction mixture over a period of hours or even minutes may significantly reduce the activity of the catalyst. This may explain why the turnover numbers reported in this study which were measured after exposure for 1/2 to 4 hours under reaction conditions are significantly lower than initial rates reported in the literature for 5% Ni/ZrO_2 (21) and 5% Ru/Al_2O_3 (22). The discrepancy between initial rates measured by Dalla Betta (21) and Vannice (22) for nickel and ruthenium catalysts might be similarly explained by differences in their pretreatment of the catalyst. Also, Vannice based his turnover numbers on CO adsorption data, which in fact may explain differences of 100-400% between his data and ours or those of Dalla Betta.

The conversions shown in Table 13 ranging from 14 to 30% are admittedly too large for differential conditions to exist. As a check for heat and mass transfer effects, two tests were performed

TABLE 13

Steady-State Activity Data for Nickel and Nickel Alloy Catalysts
275°C, 1 atm., H_2/CO = 3.5-5, GHSV = 30,000 hr^{-1}

Code	Rate		N_{CO} - Turnover # - N_{CH_4}		% Conv.		Select.
	$(\frac{\text{moles CO Conv.}}{\text{g. cat. - sec.}})^a$	$(\frac{\text{moles } CH_4 \text{ Prod.}}{\text{g. cat. - sec.}})^a$	$(\frac{\text{moles CO Conv.}}{\text{site - sec.}})^b$	$(\frac{\text{moles } CH_4 \text{ Prod}}{\text{site - sec.}})^b$	CO	CH_4	(N_{CH_4}/N_{CO})
Ni-A-111	7.56	6.3	29.8	24.8	22.0	18.2	0.83
Ni-A-114[c]	45.2	37.1	10.7	8.8	36.2	29.7	0.82
Ni-Ru-A-101	5.1	4.7	18.3	17.2	14.8	13.9	0.94
Ni-Ru-A -102	15.3	13.5	33.5	29.6	33.1	28.9	0.87
Ni-Ru-A-103	11.5	8.9	21.2	16.5	20.8	16.2	0.78
Ni-Ru-A-104	7.3	6.8	15.5	14.4	21.6	20.0	0.93
Ni-Ru-A-105#1	8.2	7.8	14.7	14.1	23.9	22.9	0.96
Ni-Ru-A-105#2	12.0	10.1	21.6	18.1	18.1	15.2	0.84
Ni-Rh-A -100#1	11.6	10.6	15.1	13.9	14.4	13.3	0.92
Ni-Rh-A -100#2[c]	23.1	21.6	30.2	28.2	14.5	13.5	0.93

0.5% Ru/Al_2O_3 Englhard Catayst Tested by Dalla Betta et al. (Ford Motor Co.) - Ref. 21	20[d]
5% Ni/ZrO_2 Dalla Betta et al. - Ref. 21	180[d]
5% Ni/Al_2O_3 M.A. Vannice (Exxon) - Ref. 22	38[d]
5% Ru/Al_2O_3 M.A. Vannice - Ref. 22	325[d]

Footnotes

a. x 10^7
b. x 10^3
c. GHSV = 60,000 hr^{-1}
d. Initial Rates

TABLE 14 Reactor Screening Data for Nickel and Nickel Alloy Catalysts
225°C, GHSV = 30,000 hr^{-1}, 16 psia

Catalyst	Conversion CO	Conversion CH_4	Production Other	Rate x 10^7 ($\frac{mole}{g\ sec}$) CH_4	Rate x 10^7 ($\frac{mole}{g\ sec}$) CO	Turnover # x 10^3 (sec^{-1}) CH_4	Turnover # x 10^3 (sec^{-1}) CO	Selectivity to CH_4
Ni-Co-A-100	16.2	15.15	1.05	9.31	9.96	4.56	4.88	0.935
Ni-Pt-A-100	16.77	15.20	1.60	9.91	10.95	4.77	5.27	0.906
Ni-Ru-A-105	5.18	3.48	1.73	2.79	4.17	3.12	4.68	0.672
Ni-Rh-A-100	3.3	2.2	1.1	1.48	2.21	1.93	2.88	0.671
Ni-Pd-A-100	6.9	6.67	0.2	4.62	4.79	2.87	2.97	0.97
Ni-MoO_3-A-101	2.9	2.5	0.4	1.83	2.11	4.07	4.69	0.87
Ni-Fe-A-100	De-activates under reaction conditions							
G-87	22.45	19.55	2.88	9.81	11.25	3.04	3.49	0.871
Ni-A-112	6.63	4.47	2.13	3.62	5.35	4.60	6.80	0.674
Ni-A-116	34.63	28.08	6.55	19.23	23.74	5.13	6.32	0.815
Ru-Pt-A-100	3.74	0.12	3.62	0.10	3.14			0.032

TABLE 15 Reactor Screening Data for Nickel and Nickel Alloy Catalysts
225°C, GHSV = 60,000 hr^{-1}, 20 psia

Catalyst	% Conversion CO	% Conversion CH_4	% Production Other	Rate x 70^7 (mole/g sec) CH_4	Rate x 70^7 (mole/g sec) CO	Turnover# x 10^3 (sec^{-1}) CH_4	Turnover# x 10^3 (sec^{-1}) CO	Selectivity to CH_4
Ni-Co-A-100								
Ni-Pt-A-100	15.53	14.03	1.43	18.47	20.33	8.88	9.80	0.903
Ni-Ru-A-105	4.15	3.25	0.88	5.23	6.63	5.87	7.44	0.788
Ni-Rh-A-100								
Ni-Pd-A-100	6.63	5.43	1.23	7.76	9.49	4.81	5.89	0.817
Ni-MoO_3-A-101	3.70	3.03	0.67	4.84	5.86	10.74	13.03	0.827
Ni-Fe-A-100	De-activates under reaction conditions							
G-87	20.37	17.43	2.93	18.53	21.63	5.75	6.72	0.856
Ni-A-112	5.70	4.63	1.03	7.12	8.71	9.04	11.05	0.812
Ni-A-116	24.05	21.98	2.05	30.88	33.76	8.47	8.99	0.914

TABLE 16 Reactor Screening Data for Nickel and Nickel Alloy Catalysts
250°C, GHSV = 30,000 hr^{-1}, 16 psia

Catalyst	% Conversion CO	% Conversion CH_4	% Production Other	Rate x 10^7 (mole/g sec) CH_4	Rate x 10^7 (mole/g sec) CO	Turnover # x 10^3 (sec^{-1}) CH_4	Turnover # x 10^3 (sec^{-1}) CO	Selectivity to CH_4
Ni-Co-A-100	46.08	35.73	10.38	22.38	28.90	10.95	14.15	0.775
Ni-Pt-A-100	30.8	30.5	0.27	19.73	19.93	9.50	9.58	0.990
Ni-Ru-A-105	10.60	8.68	1.95	6.97	8.53	7.81	9.56	0.819
Ni-Rh-A-100	8.15	5.97	2.18	4.07	5.55	5.30	7.24	0.733
Ni-Pd-A-100	15.53	13.43	2.10	9.49	10.96	5.89	6.80	0.865
Ni-MoO_3-A-101	10.2	8.8	1.35	6.50	7.50	14.40	16.65	0.863
Ni-Fe-A-100	De-activates under normal reaction conditions							
G-87	43.53	38.88	4.65	19.50	21.8	6.05	6.77	0.893
Ni-A-112	14.00	11.33	2.60	9.18	11.31	11.65	14.35	0.810
Ni-A-116	52.75	45.63	7.13	31.44	36.35	8.38	9.68	0.870
Ni-Cu-A-100	2.19	1.73	0.46	1.55	1.95			0.799

TABLE 17 Reactor Screening Data for Nickel and Nickel Alloy Catalysts
250°C, GHSV = 60,000 hr^{-1}, 20 psia

Catalyst	% Conversion CO	% Conversion CH_4	% Production Other	Rate x 10^7 (mole/g sec) CH_4	Rate x 10^7 (mole/g sec) CO	Turnover # x 10^3 (sec^{-1}) CH_4	Turnover # x 10^3 (sec^{-1}) CO	Selectivity to CH_4
Ni-Co-A-100	38.7	30.43	8.27	38.03	48.3	18.6	23.7	0.787
Ni-Pt-A-100								
Ni-Ru-A-105	9.47	8.03	1.47	12.70	14.97	14.20	16.80	0.848
Ni-Rh-A-100								
Ni-Pd-A-100	11.2	10.3	0.9	14.67	15.93	9.09	9.85	0.92
Ni-MoO_3-A-101	9.3	8.7	0.65	13.56	14.58	30.14	32.41	0.92
Ni-Fe-A-100	De-activates under reaction conditions							
G-87								
Ni-A-112	14.43	13.58	0.88	20.64	21.99	26.19	27.91	0.941
Ni-A-116	43.53	38.17	5.43	53.38	60.94	14.21	16.22	0.877

using four, then two grams of Ni-Ru- Al-105 and two tests at different space velocities for Ni-Rh-A-100. Data for these tests in Table 13 show a significant increase in the turnover number for the smaller sample and higher space velocity. These results suggest that the measured rates in Table 13 were limited by heat and mass transfer. Thus tests after the first quarter were conducted at lower conversions (some less than 10%) and at lower temperatures (225 and 250°C) to minimize such effects.

Kinetic data obtained during the second quarter are listed in Tables 14-17. For catalysts with low metal loadings, low conversions were obtained. For example, at 250°C (Tables 16 and 17) conversions for the 3 wt.% catalysts (Ni-A-112, Ni-Ru, Ni-Rh, and Ni-MoO_3) range from 4 to 14% depending upon the space velocity, whereas conversions for the 15 to 20 wt.% catalysts (all other catalysts) range from 11 to 53%. At 225°C the conversion ranges are 4 to 7% and 6 to 35% for low and high metal loadings respectively. Thus, truly differential (low conversion) conditions can be approached at 225°C for the 3% catalysts but not for the 15-20 wt.% catalysts. Apparently then, for our reactor system and for typical methanation catalysts, truly chemically-limited rate data can only be obtained for catalysts with a low metal loading (3-5 wt.%). Accordingly it would be desirable in obtaining very accurate kinetic rate data to prepare all of the catalysts with metal loadings in the 3-5% range. Nevertheless, for purposes of screening, the data obtained at moderate conversions are adequate for comparative purposes and satisfy the objectives of this study.

Apparent activation energies for some of these catalysts are shown in Table 18. With the exceptions of Ni-MoO_3-A-101, Ni-Co-A-100, and Ni-Rh-A-100, the catalysts appear to have activation energies of 12-18 kcal/mole for both CO conversion and methane formation. Ni-Co-A-100 and Ni-Rh-A-100 have slightly higher values of 22.2 and 19.2 kcal/mole respectively. Ni-MoO_3-A-101 has a significantly higher value of 26 kcal/mole which is close to the value of 25 kcal/mole for nickel reported by Vannice (22). The far right column lists the activation energies for various metals as reported by Vannice and measured under kinetic limited (low conversion) conditions. Considerably lower activation energies for alloys compared to those of either alloy component very likely result at least in part from mass transfer (or diffusional) limitations. In addition, the variations are partly the result of alloy formation, the alloy having catalytic properties different from either of the pure metals.

Vannice (22) has reported selectivities for the methanation reaction over the group VIII metals to be in the following decreasing order: Pd>Pt> Ir>Ni>Rh> Co>Fe>Ru. This order correlates well with measured selectivities for alloys of these same metals with nickel as shown in Table 19. Of special interest is Ni-Pt-A-100 which shows the highest selectivity, 99% at 250°C and higher temperatures. Changes in space velocity and temperature have appreciableeffects on the selectivity as can be seen for example in the data for Ni-A-112, Ni-Pd-A-100 and Ni-Ru-A-105. Generally the selectivity increases

TABLE 18 Apparent Activation Energies for Methanation Catalysts
Based on measurements at 225-250°C and a space velocity of 30,000 hr^{-1}

Catalyst	CO Conversion (Kcal/mole)	CH_4 Production (Kcal/mole)	Metal*	CH_4* Production Kcal/mole
Ni-Co-A-100	22.2	18.3	Co	27.0±4.4
Ni-Pt-A-100	12.4	14.3	Pt	16.3±0.8
Ni-Ru-A-105	14.8	19.0	Ru	24.2±1.2
Ni-Rh-A-100	19.2	21.1	Rh	24.0±0.4
Ni-Pd-A-100	17.1	14.8	Pd	19.7±1.6
Ni-MoO_3-A-100	26.2	26.2		
Ni-Fe-A-100			Fe	21.3±0.9
G-87	13.7	14.2	Ni	25.0±1.2
Ni-A-112	15.5	19.2		
Ni-A-116	8.8	10.2		

*Data of Al Vannice (Exxon) Ref. 19

TABLE 19 Selectivities to Methane

	250°C		225°C	
Catalyst	30,000 hr^{-1}	60,000 hr^{-1}	30,000 hr^{-1}	60,000 hr^{-1}
Ni-Co-A-100	0.775	0.787	0.935	
Ni-Pt-A-100	0.990		0.906	0.903
Ni-Ru-A-105	0.819	0.848	0.672	0.788
Ni-Rh-A-100	0.733		0.671	
Ni-Pd-A-100	0.865	0.92	0.97	0.817
Ni-MoO_3-A-101	0.863	0.93	0.87	0.827
Ni-Fe-A-100	De-activates under reactor conditions			
G-87	0.893		0.871	0.856
Ni-A-112	0.810	0.941	0.674	0.812
Ni-A-116	0.870	0.877	0.815	0.914
Ni-Cu-A-100	0.799			
Ru-Pt-A-100			0.032	

with increasing temperature for a given space velocity and with increasing space velocity for a given temperature.

Figures 17 and 18 illustrate the magnitude of the rates per gram of catalyst, the turnover numbers, and selectivities at 250°C and a space velocity of 30,000 hr^{-1}. Nominal compositions and hydrogen uptakes used to calculate turnover numbers are listed in Table 6. It should be observed that the active metal loadings which vary significantly between catalysts have an obviously marked effect on the activity of the catalyst per unit catalyst weight as can be seen in Figure 17 where the listed order corresponds to the order of wt.% active metal. A comparison of these rates with the hydrogen uptake data shows that the rate is strongly influenced by the available surface area. For example, Ni-A-116 (15 wt.% Nickel) is more active (per unit mass) than G-87 (32 wt.% nickel) mainly because the surface area of the former catalyst is larger.

Turnover numbers for 250°C and a space velocity of 30,000 hr^{-1} are shown in decreasing order of activity in Figure 18. Ni-MoO_3-A-101, Ni-A-112 (3% nickel) and Ni-Co-A-100 are the most active and G-87 the least active. The details of these results are discussed below for each catalyst.

Ni-MoO_3-A-101 has a relatively low active surface area. Thus, its rate per unit weight is among the lowest tested. However, its turnover number is the highest of any catalyst tested. Assuming a method to increase the active surface area can be found, this catalyst is a most promising candidate for further study.

Ni-Ru-A-105 and Ni-Rh-A-100 behave typically as nickel catalysts showing comparatively little effects of alloying although both are slightly less active than Ni-A-112, a nickel catalyst of comparable weight loading. The Rh does cause some increased selectivity to methane but not as pronounced as for platinum. The data determined during the past quarter show an unexpectedly low selectivity to methane for Ni-Rh. Thus, some of these runs will be repeated.

Ni-Co-A-100 contains a high loading of metal with equal weight percents of nickel and cobalt. It is of special interest in that both the rate per unit weight and the turnover number are high. The selectivity of this catalyst for the methanation reaction (78% at 250°C and GHSV = 30,000) is the lowest of any nickel catalyst tested. Vannice (22) has reported cobalt to have a selectivity of 78% under similar reaction conditions and the selectivity for nickel to be 90% also in good agreement with our data. Thus, cobalt has a strong effect on the selectivity of the Ni-Co catalyst. Nevertheless, a recent test during the past quarter showed the same catalyst to have a 93.5% selectivity at 225°C and GHSV= 30,000 hr^{-1}. Since the selectivity should be lower at 225 than at 250°C, these data must be repeated.

Ni-Fe-A-100 was found to completely deactivate within two hours under normal reactor operating conditions. When the catalyst

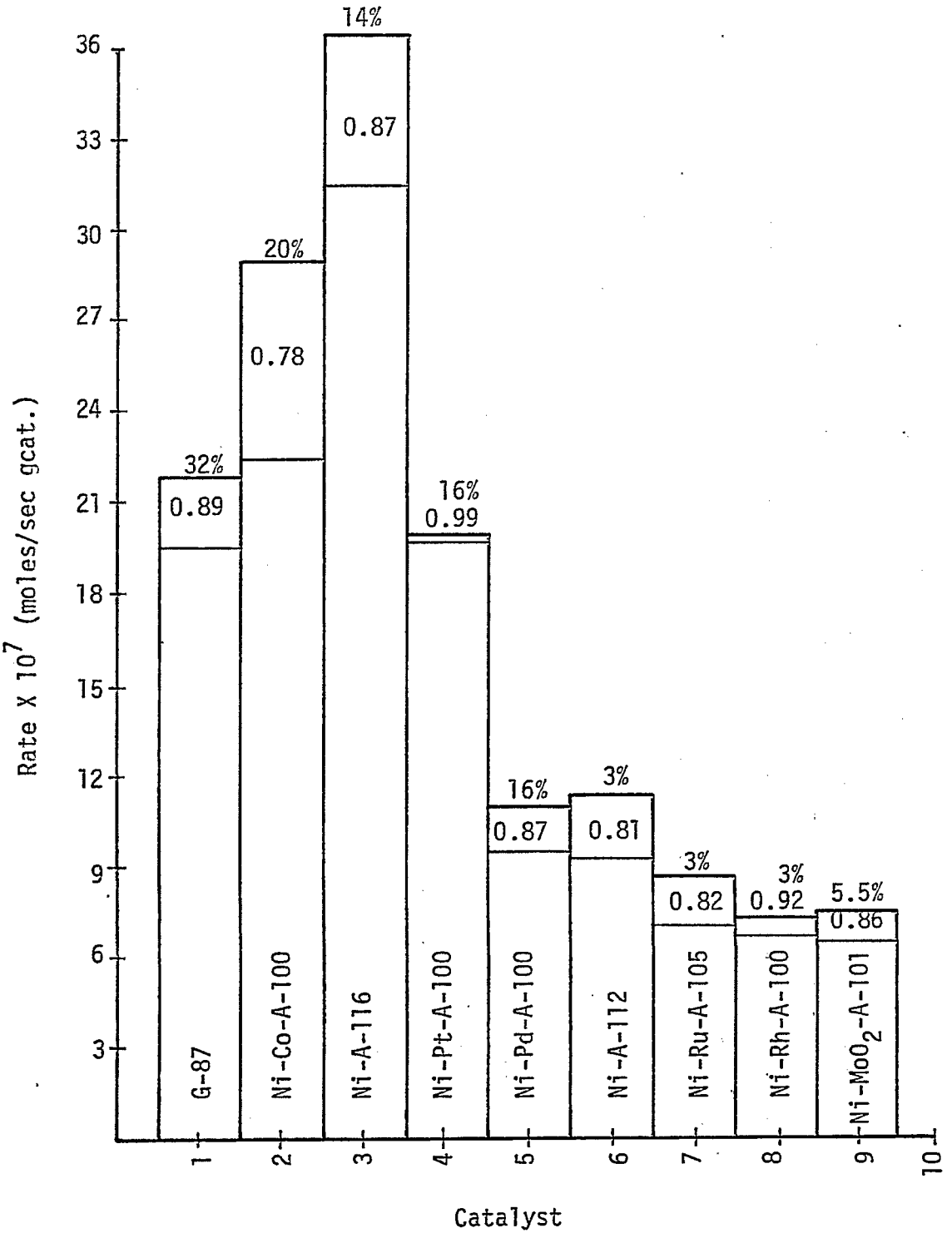

Figure 17. Specific Methanation Rates (mass basis) for Nickel and Nickel Alloy Catalysts. (Percentages are active metal loadings. Fractions represent selectivity to methane.) (GHSV = 30,000 hr^{-1}, 250°C, 1 atm)

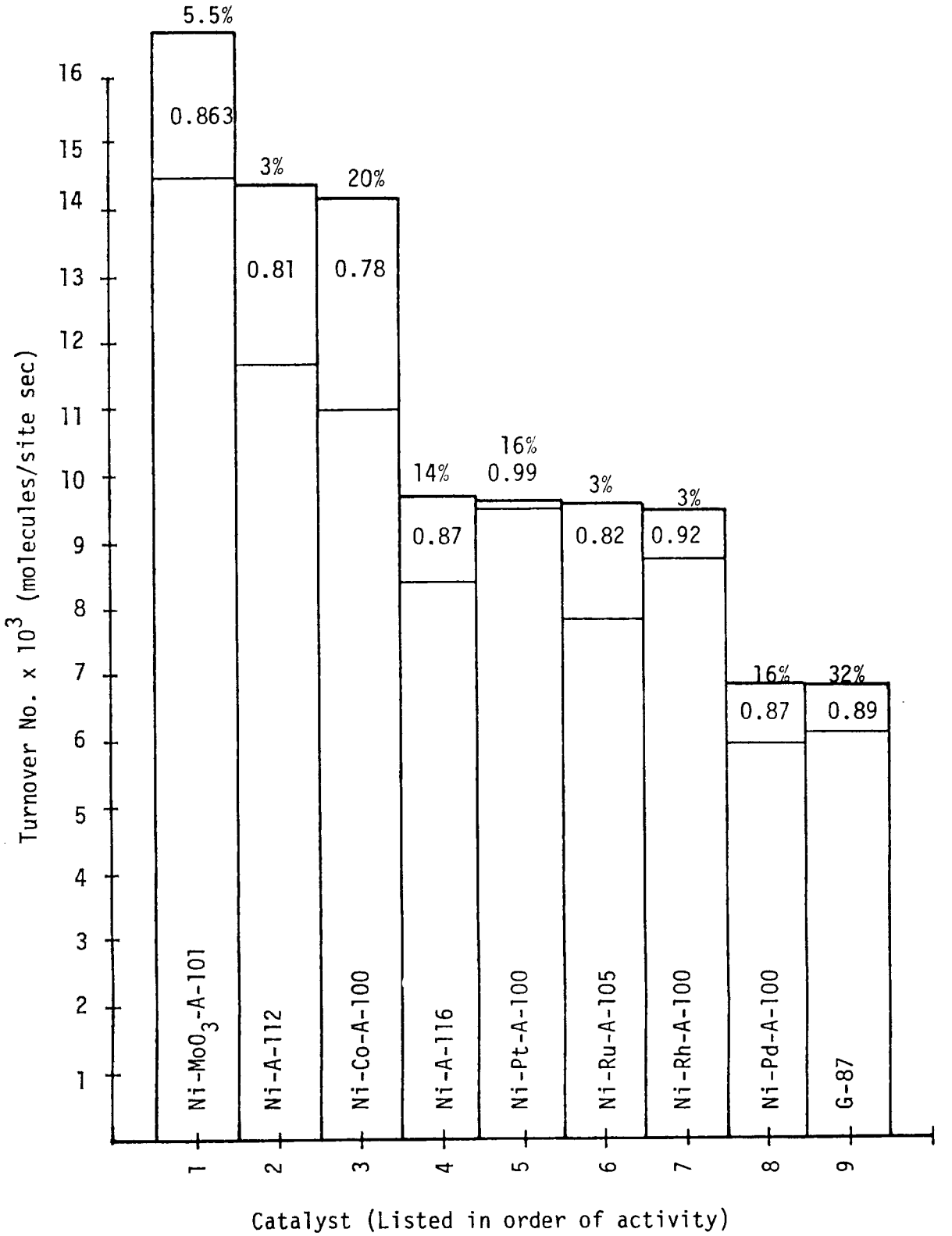

Figure 18. Turnover Numbers (molecules product/site sec) for Methanation on Nickel and Nickel Alloy Catalysts. (Percentages are active metal loadings. Fractions represent selectivity to methane.) (GHSV = 30,000 hr^{-1}, 250°C, 1 atm)

was removed from the reactor some of the beads showed a brown (rust) color as compared to the normal black. The observations suggest that the iron may scavange the oxygen from the CO to form various iron oxides and thus effectively poison the catalyst. It is also possible that the Ni-Fe catalysts was not completely reduced at the beginning of the test (4). Additional reactor and x-ray tests are planned to investigate these possibilities.

Ni-Pd-A-100 was found to be less active than most of the alloys tested thus far with a turnover number about the same as G-87.

Ni-Pt-A-100 has rate characteristics which are not outstandingly different from the other catalysts. The selectivity, however, is significantly improved over nickel. Vannice (22) has shown platinum to be one of the most selective catalysts for methane--namely about 98% to CH_4. As an alloy with nickel in the amount of only one atomic percent platinum continues to effect a 99% selectivity to methane.

Ni-A-116 is a high loading (15 wt.%) nickel catalyst used to compare against other catalysts containing 15-20 wt.% metal. It has the highest rate per unit weight but has a turnover number the same as Ni-Pt-A-100 and somewhat lower than the cobalt alloy.

G-87 is a commercial nickel catalyst manufactured by Girdler Catalyst Corp. and is included as a comparison against other nickel catalysts. It is unique, however, from the other catalysts tested because it contains a different support of unknown composition which may influence the diffusional and mass transfer characteristics of the catalyst. Because of its high nickel loading (32 wt.%) it is expected that its rate per unit weight should be high. However, its turnover number is one of the lowest measured. This may be due in part to the effects of pore diffusion resistance at a relatively high conversion of CO.

Reliable data on Ni-Cu-A-100 (see Table 16) were obtained at 250°C and a space velocity of 30,000 hr^{-1}. This is the least active catalyst tested thus far also showing relatively low selectivity. No further work is expected to be done with this catalyst because of its low activity.

Ru-Pt-A-100 is 0.5% Ru, 0.5% Pt by weight. Reliable data for this catalyst were obtained at 225°C and a space velocity of 30,000 hr^{-1}. The results suggest a low activity, very low selectivity catalyst. Nevertheless, the H_2 uptake must be determined in order to determine if the turnover number is large or small. It should also be important to determine the activity at 250 or 275°C.

b. Effects of passivation on activity and integral tests for Ni-A-114 and G-87. A test was conducted to determine the effects of passivation on a nickel catalyst which was prepared in our NSF

study. A 20-gram sample of Ni-A-114, 15% nickel on alumina was used. The catalyst was reduced and pretreated in the usual manner, after which an integral test was carried out. The catalyst was then passivated with a 1% air in N_2 stream at a space velocity of about 15,000 hr^{-1}. The leading edge of the bed experienced a 12°C temperature rise which lasted about 5 minutes. The trailing edge experienced a rise of 25°C over about 10 minutes. The catalyst was again reduced followed by another integral test. The catalyst was again passivated in the same manner as previously and very similar temperature effects were noted.

Conversion versus temperature data are plotted in Figure 19 for the two integral tests described above. Conversion versus temperature curves are very similar for both runs and reach a maximum between 275°C and 300°C. Approximately 90% of the CO usage is accounted for by CH_4 production. The remainder may be assumed to have been converted to CO_2 and other hydrocarbons.

An integral test was also carried out for G-87 (Girdler) for which the conversion versus temperature data are shown in Figure 20. A maximum methane production of 80% is obtained for G-87 compared to 90% for Ni-A-114 (see Fig. 19). This lower production for methane for the commercial catalyst may be a result of unreduced NiO present in the catalyst which is known (24) to be an effective catalyst for the decomposition of methane: $CH_4 + H_2O = CO + 3H_2$, thus retarding the ultimate conversion to methane. Ni-A-114 was prepared in such a manner as to maximize nickel metal formation and minimize formation of NiO.

3. Work Forecast. Catalyst screening is in full progress and will continue through May and June. Screening tests for alumina-supported Ru, Ru-Pt, Ru-Pd, Ru-Co, and Ni-Cu will be carried out at 225 and 250°C. Alumina-supported Ni-MoO_3, Ni-Ru, Ni-Rh, Ni-Fe, Ni-Co, Ni-Pt, Ni-Pd, Ni, Ru-Pd, Ru-Co, and selected industrial methanation catalysts will be screened after exposure to 10 ppm H_2S.

D. Task 4: Catalyst Geometry Testing and Design

This task is formerly scheduled to begin 18 months after initiation of the project or in other words October 22, 1976. No experimental work was completed during the past year, however, some early work with monolithic nickel and nickel alloys is tentatively scheduled for the next quarter in connection with this task. Arrangements have been made with technical and sales representatives of Corning Glass Works in which they will send us monolithic supports of various geometries. In fact, some of these samples have already been received by our laboratory. The possibility of testing one or two samples of sprayed-Raney-nickel catalyst of the parallel plate configuration has also been discussed with technical representatives at the Pittsburgh Energy Research Center in Pittsburgh.

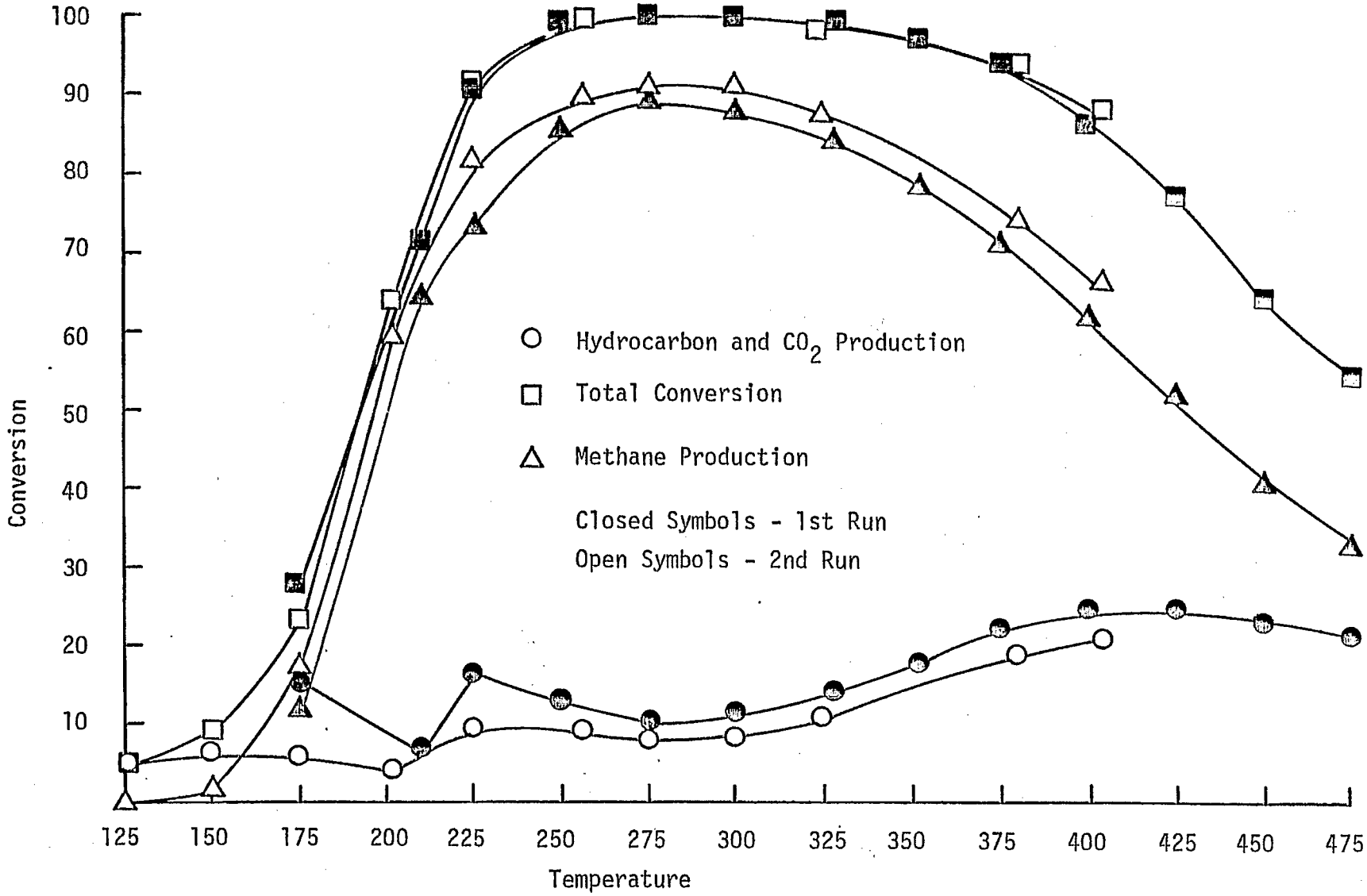

Figure 19. Integral Activity Test For Ni-A-114 (15% Ni/Al_2O_3)
(GHSV = 15,000 hr^{-1})

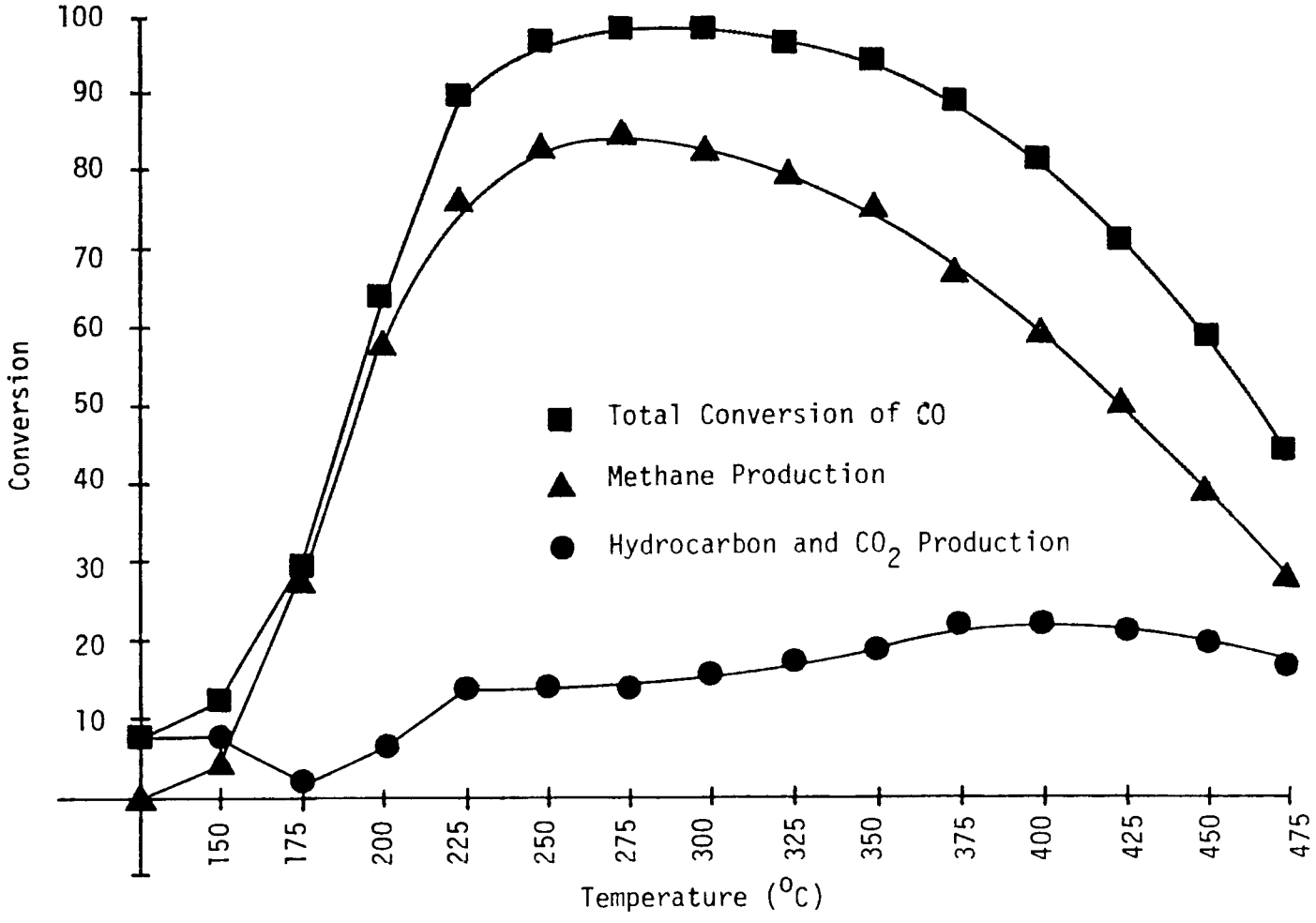

Figure 20. Integral Activity Test for G-87 (Girdler) Nickel Catalyst
Space velocity = $15{,}000_3 hr^{-1}$
Catalyst volume = 35 cm^3
Reactant mixture: 1% CO, 4 H_2, 95% N_2

E. Task 5: Technical Visits and Communication

1. Accomplishments. During the past several months the principal investigator has established technical communications with other workers active in methanation catalysis, many of whom are listed on the Report Distribution List in Appendix B. Private communications in the form of letters, phone calls, exchange of preprints, and informal discussions at meetings have been very helpful in keeping up-to-date and comparing important results while avoiding unnecessary duplication of others' research.

The principal investigator has been Secretary-Treasurer of the California Catalysis Society during the past year and is presently the Task Force Leader for Metal Surface Areas on the ASTM D-32 Catalyst Committee. These professional duties bring the principal investigator directly in contact with others working in catalyst characterization, surface area measurement, and methanation catalysis, all pertinent to this present investigation.

A particularly profitable learning experience at the beginning of the first quarter involved attendance by the principal investigator at the Symposium on Catalytic Conversion of Coal held April 21-23, 1975 in Pittsburgh. The experience was valuable in terms of direct private contacts and communications with other workers in methanation catalysis and informative presentations dealing directly with methanation catalysis and other catalytic aspects of coal conversion.

During the second quarter the principal investigator and Mr. Kyung Sup Chung attended the ERDA/EPRI/NSF-RANN Contractors Conference held October 22-23, 1975 in Park City, Utah. The experience was very profitable because of direct private conversations with other workers in coal conversion and informative presentations outlining other coal conversion projects. Preliminary arrangements to visit other laboratories were initiated during this meeting.

During the third quarter the principal investigator attended the California Catalysis Society Meeting held November 7-8, 1975 in Pasadena where he engaged in fruitful discussions with other investigators in regards to hydrogen and carbon monoxide chemisorption on nickel. The PI also presented a paper "Chemistry of Nickel-Alumina Catalysts" at the 68th Annual AIChE meeting in Los Angeles held November 16-22, 1975 and attended a short course dealing with "Catalyst Deactivation." The short course was rigorous, informative and quite pertinent to our present poisoning work.

Dr. Bartholomew was symposium chairman for the First Rocky Mountain Fuel Symposium held January 30, 1976 at Brigham Young University. Approximately 170 professionals and students attended the all-day meeting which was split into two technical sessions for most of the day. The symposium featured 24 different speakers in discussions of coal gasification, oil shale, and tar sand research and development. Mr. Blaine Barton presented some of our kinetic data in a talk entitled

"Alloy Catalysts for Methanation of Coal Synthesis Gas." Our luncheon speaker, Senator Frank Moss of Utah, discussed the political aspects of fuel development in the West. Feedback in regard to the symposium has been quite favorable and the prospects are very good for a 2nd Rocky Mountain Fuel Symposium next year and formation of a Rocky Mountain Fuel Society.

During the fourth quarter, the principal investigator, Mr. Joseph Oliphant, and Mr. Richard Pannell (both students supported by NSF) attended the Spring Meeting of the California Catalysis Society where Mr. Pannell presented a paper dealing with H_2 and CO adsorption on nickel powder. Dr. Bartholomew has also participated in the organization of the new Utah Consortium for Energy Research and is involved as a member of the catalysis committee. The committee has plans to prepare joint University of Utah-BYU proposals in the Fossil Fuels area and to organize a center of excellence in catalysis.

2. Forecast. During the coming quarter, the principal investigator will visit methanation laboratories at IGT, Carnegie-Mellon University, and the Pittsburgh Energy Research Center (May 11-14) , will attend the ASTM Meeting in Gaithersburg, Md. (May 17-18), and will visit with ERDA officials in Washington (May 19) and at BYU (May 12). Dr. Bartholomew will also attend the Gordon Conference on Catalysis in New Hampshire June 28-July 2. The PI will continue participation on the catalysis committee of the Utah Energy Consortium. During the summer, the catalysis laboratory will prepare and submit a continuation proposal for this project.

F. New Publications and Personnel

Mr. Kyung Sup Chung completed work on his master's thesis entitled, "The Effects of H_2S Poisoning on Hydrogen and Carbon Monoxide Chemisorption on Nickel and Nickel Alloys." Mr. Chung has already begun work at the University of Utah (Department of Mining, Metallurgical, and Fuels Engineering) toward a PhD and successfully completed his oral examination on February 19. Mr. Richard Fowler, a junior in Chemical Engineering joined our research group in January.

IV. CONCLUSIONS

A. In preparation of monolithic catalysts, a 2.5:1 or 3:1 slurry of water and SA Medium Al_2O_3 gives the maximum coating in the smallest number of dips. Impregnation with a $Ni(NO_3)_2\ 6H_2O$ melt or with a 50 wt.% aqueous solution of $Ni(NO_3)_2\ 6H_2O$ maximizes the nickel loading with a minimum number of applications. Either impregnation technique results in about the same surface area.

B. In a 3% Ni-Mo/Al_2O_3 catalyst, the nickel sites adsorb both H_2 and CO, whereas the MoO_3 sites do not.

C. Alumina-supported nickel alloys have dispersions which are about the same on less than Ni/Al_2O_3. Ruthenium catalysts in the 0.5 wt.% range have higher dispersions than 3% nickel catalysts.

D. Carbon monoxide adsorption on nickel is an unreliable technique for measuring nickel surface area in view of (1) considerable variation in adsorption uptakes resulting from modest variations in equilibration pressure and temperature, (2) formation of $Ni(CO)_4$ causing significant loss of nickel from the catalyst, and (3) extensive physical and chemical adsorption of carbon monoxide on the alumina support requiring large corrections to the data with corresponding losses in accuracy.

E. Significant quantities of carbon monoxide are chem-and physisorbed on Al_2O_3 at both 25 and -85°C. Hydrogen adsorption (chemical or physical) on Al_2O_3 is negligible at 25°C.

F. Values of CO/H generally range from 1.5-2.0 for alumina-supported nickel alloy catalysts suggesting the formation of surface metal carbonyls during CO adsorption or possibly CO spillover to the support.

G. Data for CO adsorption on a nickel powder at 25°C show a CO/H value of 1.74 suggesting surface carbonyl formation. After evacuation at 25°C, however, the ratio decreases to 0.76, showing that reversible adsorption-desorption occurs. A value of CO/H of 0.76 is also obtained at -83°C before and after pumping at the low temperature indicating no reversible adsorption. Our procedure of measuring CO adsorption at -83°C avoids complications due to either carbonyl formation or reversible CO adsorption.

H. The effects of H_2S poisoning on a catalyst depend upon catalyst loading, H_2S/H_2 space velocity and concentration and temperature of exposure. If poisoning effects are to be compared between catalysts, these parameters must be fixed. The poisoning ratio is a convenient quantitative means for comparing resistance to poisoning between catalysts in terms of adsorption capacity.

I. The observed decrease in hydrogen adsorption for a catalyst after exposure to 10 ppm H_2S for 12 hours is a qualitative measure of its resistance to sulfur poisoning. The order of decreasing resistance to poisoning for catalysts studied thus far is: Ni-Rh Ni-Ru Ni Ni-MoO_3 Ru. However, Ni-MoO_3/Al_2O_3 shows unusual behavior by adsorbing within 3-6 hours enough H_2S to block 40-45% of the hydrogen adsorption sites after which there is no further significant adsorption of H_2S within the next 6-12 hours. Ni-Pd, Ni-Co, and Pd-Ru catalysts have low poisoning ratios indicating reasonably high resistance to sulfur poisoning in terms of adsorption capacity.

J. The increase in carbon monoxide adsorption after exposure to H_2S may be explained by the formation of a COS or $(CO)_xS$ complex which after formation migrates to the support.

K. X-ray diffraction measurements to determine phase composition and crystallite sizes of alumina-supported nickel and nickel alloys are feasible if a sensitive instrument is available and if the signal-to-noise ratio is increased by running at very slow rate or by counting at fixed angles. Diffraction data for nickel and ruthenium alloys suggest that the metals are probably in solid solution (i.e. exist as alloys). Particle sizes calculated from x-ray line broadening are generally smaller than those calculated from hydrogen chemisorption data for nickel and nickel alloys. This observation may be explained by considering that some of the nickel or other metal sites are not reduced completely to the metal.

L. Steady-state conversions of carbon monoxide at 275°C, 1 atm. (inlet composition of 1% CO, 4% H_2, 95% N_2) range from 14-35% for alumina-supported Ni-Rh, Ni-Ru and Ni. Percent selectivities to methane range from 78-94%. Turnover numbers are not significantly different within experimental error for these catalysts and compare favorably with initial rates reported for 5% Ni/Al_2O_3 and 0.5% Ru/Al_2O_3.

M. Steady-state conversion measured at 225 and 250°C, 1 atm and for space velocities of 30,000 and 60,000 hr^{-1} indicate that very nearly differential (low conversion) conditions obtain only for low (3-6 wt.%) metal loading catalysts. Screening data for 15-20 wt.% metal/Al_2O_3 catalysts are influenced by mass transfer or diffusional limitations.

N. Ni-MoO_3/Al_2O_3 is the most active catalyst on a per surface area basis. Ni-Pt/Al_2O_3 has the highest selectivity for methane production--namely 99% (250°C, 30,000 hr^{-1}). A 15 wt.% Ni/Al_2O_3 is the most active catalyst on a per mass basis--even more active than a commercial 32 wt.% Ni/Al_2O_3 simply because the 15% catalyst has a high nickel surface area.

O. Conversion versus temperature data indicate that a commercial nickel catalyst attains a maximum methane production of 80% at 250-

300°C compared to a production of 90% for a 15 wt.% Ni/Al_2O_3 prepared in this laboratory. The higher selectivity for the latter catalyst is possibly a result of its higher state of reduction to metallic nickel.

V. REFERENCES

1. M. Greyson, "Methanation" in "Catalysis" Vol. IV, ed. P.H. Emmett, Rheinhold Pub. Corp., New York, 1956.

2. G.A. Mills and F.W. Steffgen, "Catalytic Methanation," Catalysis Reviews 8, 159 (1973).

3. C.H. Bartholomew, "Alloy Catalysts with Monolith Supports for Methanation of Coal-Derived Gases," Quarterly Technical Progress Report FE-1790-1 (ERDA), Aug. 6, 1975.

4. C.H. Bartholomew, "Alloy Catalysts with Monolith Supports for Methanation of Coal-Derived Gases," Quarterly Technical Progress Report FE-1790-2 (ERDA), Nov. 6, 1975.

5. C.H. Bartholomew, "Alloy Catalysts with Monolith Supports for Methanation of Coal-Derived Gases," Quarterly Technical Progress Report FE-1790-3 (ERDA) Feb. 6, 1976.

6. R.J. Farrauto, "Determination of Catalytic Surface Area Measurements," AIChE Symposium Series, 70, No. 143, 9-22 (1975).

7. C.H. Bartholomew and R.J. Farrauto, "Chemistry of Ni/Al_2O_3 Catalysts," presented at the 68th Annual AIChE Meeting, November 16-20, 1975, Los Angeles; submitted to the Journal of Catalysis.

8. C.H. Bartholomew, "New Catalysts for Methanation," NSF Study in Progress, ENG75-00254.

9. C.H. Bartholomew and M. Boudart, "Surface Composition and Chemistry of Supported Platinum-Iron Alloys," J. Catal. 29, 278 (1973).

10. C.E. O'Neill, Ph.D. Thesis, Columbia University, 1961.

11. A.W. Alday, and L.D. Schmidt, J. Catal., 22, 260 (1971).

12. J.J.F. Scholten, and A. Van Montfoort, J. Catal., 1, 85 (1962).

13. J. Freel, J. Catal., 25, 149 (1972).

14. T.A. Dorling, and R.L. Moss, J. Catal., 7, 378 (1967).

15. D. Cormack, and R.L. Moss, J. Catal., 13, 1 (1969).

16. J.R. Rostrup-Nielsen, J. Catal., 2, 222 (1968).

17. R.B. Anderson, L.J.E. Hofer, F.S. Karn, and J.F. Shultz, J. Phys. Chem. 66, 501 (1962).

18. J.E. Benson, M. Boudart, and H.S. Hwang, J. Catal., 39, 44 (1975).

19. W.B. Pearson, "A Handbook of Lattice Spacings and Structures of Metals and Alloys," Pergamon Press, New York, N.Y. (1956).

20. H.P. Klug and L.E. Alexander, "X-ray Diffraction Procedures," John Wiley, New York, 1954.

21. R.A. Dalla Betta, A.G. Piken, and M. Shelef, "Heterogeneous Methanation: Initial Rate of CO Hydrogenation on Supported Ruthenium and Nickel," J. Catal., 35, 54 (1974).

22. M.A. Vannice, "The Catalytic Synthesis of Hydrocarbons from H_2/CO Mixtures Over the Group VIII Metals," J. Catal., 37, 449 (1975).

23. R.A. Dalla Betta, A.G. Piken, and M. Shelef, "Heterogeneous Methanation: Steady-state Rate of CO Hydrogenation on Supported Ruthenium, Nickel, and Rhenium," submitted to J. Catal.

24. C.L. Thomas, "Catalytic Processes and Proven Catalysts," Academic Press, New York, 1970, p. 101.

APPENDICES

A. PLANAR DENSITIES FOR ALLOYS AND PURE METALS

B. REPORT DISTRIBUTION LIST

C. BIBLIOGRAPHIC DATA SHEET

TABLE 1A Catalyst Composition & Planar Densities

Catalyst	Metal Loading (Wt.%)	Metal Composition (atomic %)	Planar Density Å/atom
Ni-Fe-A-100	10% Fe 10% Ni	51.25% Fe 48.75% Ni	5.30
Ni-Co-A-100	10% Co 10% Ni	49.99% Co 50.01% Ni	6.90
Ni-Pd-A-100	15% Ni 1% Pd	96.45% Ni 3.55% Pd	6.82
Ni-Pt-A-100	15% Ni .5% Pt	98.87% Ni 1.12% Pt	6.79
Ru-Co-A-100	15% Co .52% Ru	98% Co 2% Ru	7.07
Ru-Pd-A-100	.513% Pd .487% Ru	50% Ru 50% Pd	8.21

TABLE 2A Planar Density Summary

Metal	Crystalline Form	Planar Density A^2/atom	Source
Ni	FCC	6.77	Arithmetical average of (100), (110), and (111) planes
Fe	BCC	3.90	Arithmetical average of (100), (110), and (111) planes
Pd	FCC	8.24	Arithmetical average of (100), (110), and (111) planes
Pt	FCC	8.39	Arithmetical average of (100), (110) and (111) plantes
Ru	HCP	8.17	Arithmetical average of (100), (001), and (101) planes
Co	HCP	7.05	Arithmetical average of (100), (001), and (101) planes

U.S. DEPARTMENT OF COMMERCE
Technology Administration
National Technical Information Service
Springfield, VA 22161 (703) 605-6000